Design of a Minimal Invasive Sentinel Lymph Node Biopsy Device

TU Delft

Jun 2024
Aart Mommersteeg

Design of a Minimal Invasive Sentinel Lymph Node Biopsy Device

Actuating a locally expanding adaptable cutting blade

by

A.J. (Aart) Mommersteeg

Student number:	4593871
Faculty:	Faculty of Mechanical Engineering, Delft
Thesis committee:	Prof.dr. J.J. (John) van den Dobbelsteen
	Dr. D.J. (Dirk) Grünhagen
	A.W. (Teun) Schurink

TU Delft

Preface

The following thesis is the final project before completing the Master of Mechanical Engineering at the TU Delft. I have had the chance to continue research of the TU Delft and the Erasmus MC regarding the design and development of a minimal invasive sentinel lymph node biopsy device. This project has been a new experience, one with challenges but also opportunities to learn and experience new things, something which I very much enjoyed. The following chapters will guide you through each phase of the project, illustrating the steps taken and the thoughts behind the decisions made. From the initial design to the final testing, you will see how the project evolved and the insights gained along the way. A special thanks to Teun, John, Dirk, Annika and Pien for the opportunity, great guidance and support throughout this project.

A.J. (Aart) Mommersteeg
Delft, June 2024

Contents

1
Introduction

The following thesis explores the feasibility of a minimally invasive biopsy device to replace or be used in the currently existing sentinel lymph node biopsy (SLNB) procedure. This thesis describes the full designing process and testing phase to investigate weather such a device can be used to improve the current biopsy procedure. To give some background information and familiarise the reader, an introduction into SLNB is given below after which the possible advantages of a minimal invasive sentinel lymph node biopsy device (MISLNBD) are highlighted. After this, the research objective and a full thesis overview are presented.

1.1. Sentinel Lymph Node Biopsy

SLNB is used as a staging method for patients diagnosed with cutaneous malignant melanoma, a type of skin cancer. Accurate staging is crucial for predicting the extent of the disease's progression and determining suitable therapy for the patient [1], [2], [3].

1.1.1. SLNB characteristics

Melanoma is known to spread via the lymphatic system, first metastasising the sentinel lymph nodes (SLN's). SLN's are the lymph nodes directly affected by the primary tumour drainage and are therefore highly likely to be the first nodes to show metastasis [4]. SLNB consists of locating and removing the SLN's after which they can be inspected for metastasis by means of a pathological evaluation [5].

Since the SLN's are directly fed by the tumour drainage, the remaining LNs in the relevant primary and subsequent basins have a high probability to be free of malignant cells when the SLN's test negative after pathological evaluation. When the tested SLN contains metastasis however, the malignant cells have likely spread past the sentinel nodes through the patients lymphatic system, resulting in a stage III melanoma according to the eighth edition AJCC TNM [6]. Recent advancements in the availability of effective adjuvant targeted and immune systemic therapies for stage III melanoma empathise the need for accurate staging techniques to form a suitable treatment strategy. There are non-invasive staging methods available like x-rays, blood tests, CT-scans, MRI, and PET-scans but these rely on dimensional and visual guidelines. The pathological evaluation of the SLN can provide direct observation of present malignant cells and therefore, proves to be highly reliable compared to these non-invasive options. SLNB is offered to cutaneous melanoma patients with a high risk of metastasis but without clinical evidence of LN involvement [5], [7], [8], [9]. Due to the need for surgical removal of the SLN, complications of SLNB include: bleeding, nerve injury, scar formations, infections and lymphedema. Partly because SLNB is offered to patients with clinically negtive LNs, around 80% of patients who undergo an SLNB procedure test negative for metastasis [4], [8].

The high reliability of the SLNB procedure compared to the potential complications and low likelihood of a positive prognosis creates a trade-off that requires careful risk assessment for each patient. Improvement of the current SLNB procedure can positively shift this trade-off in favour of the patient.

1.1.2. Current SLNB procedure

The SLNB procedure starts with a lymphoscintigraphy, a nuclear lymphatic mapping to identify the locations of one or more SLN's. Lymphoscintigraphy involves intradermal injection of technetium-99m (^{99m}Tc), a radiotracer of a radioactive isotope commonly used in nuclear medicine imaging procedures. The (^{99m}Tc) filtered sulphur colloid is injected at the primary melanoma site, the SLN's draining from this area around the tumour will cause the (^{99m}Tc) to migrate. The (^{99m}Tc) therefore marks the SLN's making them detectable by a gamma camera or probe [10]. Before the operative procedure in the operating room (OR), the patient undergoes general anaesthesia. The general direction of the target SLN is determined and incisions are made to create a path through the skin towards the SLN. After identification with the gamma probe, the SLN is manually dissected from surrounding tissue and harvested for pathological evaluation [8]. During SLNB, it is important to excise the lymph node in its entirety (en-bloc), to ensure the detection of all potential metastatic deposits and to prevent any leakage thereof [11]. The SLNB procedure can be divided in four different steps: A - Nuclear mapping and target identification. B - Localisation of SLN. C - SLN excision. D - Wound care [12]. An illustration of this first 3 steps can be found in figure 1.1.

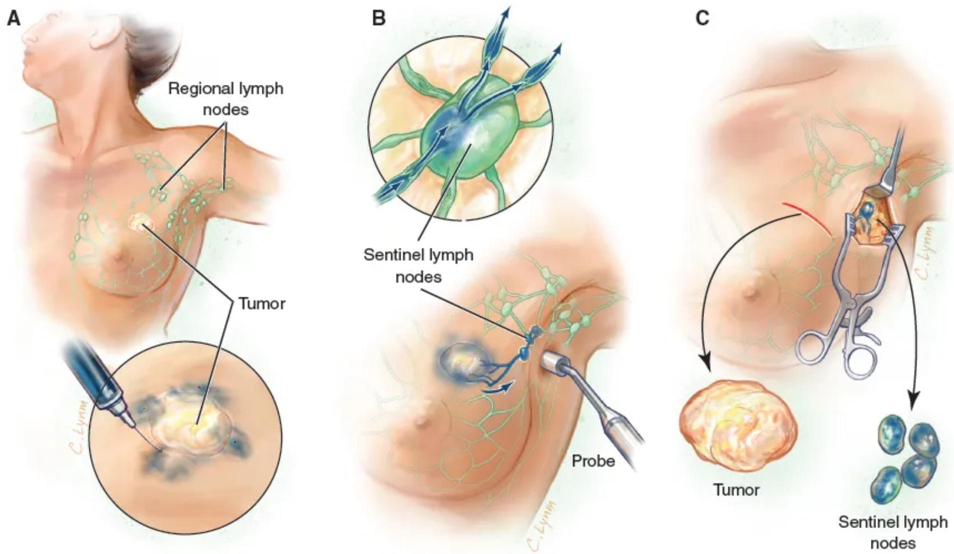

Figure 1.1: A - Radioactive isotope and/or blue dye is injected into the tissue surrounding the tumor. B - The injected material migrates to draining lymph nodes. Sentinel nodes are identified visually or with a gamma-detecting probe. C - The tumor and sentinel nodes are excised for pathologic assessment of the regional lymph nodes. Figure and caption found in [12].

1.2. Minimally invasive sentinel lymph node biopsy device

Collaborative research performed by TU Delft and Erasmus MC Rotterdam, investigates the possibility of integrating a minimal invasive biopsy device during the SLNB procedure. The use of a MISLNBD looks to potentially improve step *C - SLN excision* by exchanging the manual use of a scalpel or monopolar cutting tool with the following device actions. The device is inserted and positioned in the correct location via a minimally invasive incision through the skin. A separation mechanism present in the device will separate the target LN from surrounding tissue. After separation, the device is removed while simultaneously harvesting the LN for pathological evaluation. This eliminates the need to manually create an access route to the target LN. Incisions in skin will be smaller while actuation of these steps is controlled from outside of the patients body. This had the potential to greatly reduce the overall tissue damage experienced by the patient. A reduced footprint presents opportunities to eliminate the necessity for general anaesthesia, opting instead for the use of local anaesthesia only. Local anaesthesia can reduce the impact of the procedure and reduce recovery time for the patient, while also eliminating the need for an anaesthetist and therefore an OR. Avoiding the demands of an OR schedule creates a more time-efficient and cost-effective procedure, which is particularly valuable during events such as the recent COVID-19 pandemic where surgeries had to be postponed or cancelled.

1.3. Research objective

Previous research conducted by M.I. Joosen [13] and L.R. Preis [14] investigated different extraction techniques that could potentially be used in the design of a MISLNBD. Continuing on the fundamental research done by Joosen, Preis has shown great potential in the use of an expandable ring shaped cutter as the main cutting mechanism to separate the SLN from surrounding tissue. After a minimally invasive insertion of the device, the hollow ring shaped cutter needs to be expanded to accommodate the removal of the entire lymph node, which diameter is larger than the initial insertion diameter. After expansion based on the size of the SLN, the device is pushed forwards, generating a cut around the target SLN. However, technical challenges arise when expanding such a device inside of the patients body while maintaining these minimally invasive properties. A sturdy support for the ring is required while the small incision size limits the available space that can be used to actuate such an expansion.

This thesis builds upon the research conducted by Joosen and Preis, aiming to explore the possibility of developing a MISLNBD. The focus will be on designing and testing a new device based on an expandable cutting ring, with particular attention the the actuation and support mechanisms required for such an expansion. Preceding this thesis, a comprehensive literature review was conducted to explore existing expansion techniques. Various mechanisms were analysed to identify potential candidates for integration in to the design of the new MISLNBD. [15] In this thesis, different conceptual frameworks will be proposed and evaluated, leading to the presentation of a finalised design for testing and refinements as a potentially new MISLNBD.

2
Device conceptualization

To guide the design process, assumptions are listed below followed by a set of functional requirements and selection criteria. The functional requirements represent a set of strict constraints that the design needs to adhere to, ensuring its functionality. In contrast, the selection criteria provide a framework for comparing and evaluating different concepts. Following this, three concepts will be presented, each of which will be graded against the selection criteria to determine the most suitable option for this research.

2.1. Assumptions and functional requirements

The main function of a MISLNBD will be to replace and improve step *C - SLN excision* of the current SLNB procedure. Both step *A - Nuclear mapping and target identification* and step *B - Localisation of target* are assumed to remain unchanged during implementation of this device, and are therefore assumed outside the scope of this thesis. Even though the wound shape or after care might be different, the procedure of step *D - After care* will also be relatively unchanged and therefore not be the focus of this project.

The SLN's are assumed to be ellipsoidal in shape. Research indicates that both benign (malignant-free) and malignant lymph nodes typically range from 12 to 22mm in length for the long axis and 5 to 15mm for the short axis, with mean diameters averaging 1.7mm and 1mm, respectively [16]. The orientation of any SLN with respect to the device is assumed to be variable, given the nature of the lymphatic system and the limited approach angle imposed by surrounding muscle and bone structures. The depth of the SLN beneath the skin surface is also variable for each patient and among individual nodes, a depth ranging between 14 to 80mm is assumed, averaging a depth of 43mm [17].
In summary, the following assumptions are made:

- Identification and localisation of SLN is done prior to the use of the device.
- Positioning of device can be done accurately relative to target SLN.
- SLN shape is ellipsoid with size ranging from 12 to 22mm for long axis and 5 to 15mm for short axis. Averaging 1.7 and 1mm respectively.
- Average SLN depth of 43mm.
- SLN can be present in any orientation.

Next to these assumptions, functional requirements are set up to which a design must adhere to. Maintaining the SLN's structural integrity is essential for accurate pathological evaluation and serves to prevent potential leakage of melanoma cells into other parts of the patients body. This is why the MISLNBD must be able to excise the SLN en-bloc, without breaching its integrity during the SLNB procedure. Furthermore, the device needs to be adaptable, in order to accommodate any of the assumed SLN's which vary in location, orientation and size. Finally, for the device to be used inside a patient, bio-compatible and sterilizable materials may exclusively be used.

A summary of the functional requirements is shown below.

- LN must me extracted en-bloc, integrity of LN may not be breached.
- Must be able to separate and extract differently sized and oriented LN for any of the assumed LN sizes.
- Material must be bio-compatible and sterilizable

2.2. Concept presentation

With the use of these assumptions and functional requirements, three different concepts are created. They will be presented and explained in the sections below. Each concept follows five steps to form the excision during the SLNB procedure, *1) Positioning, 2) Expansion, 3) Cutting, 4) Separation* and *5) Retrieval*. Due to the variable orientation of the SLN, it is being illustrated as a spherical object in the following concepts.

2.2.1. Concept - Rotating rods

The first concept makes use of a locally expandable cutting blade inside the patient, different steps for the desired excision process are explained below and an overview can be found in figure 2.1.

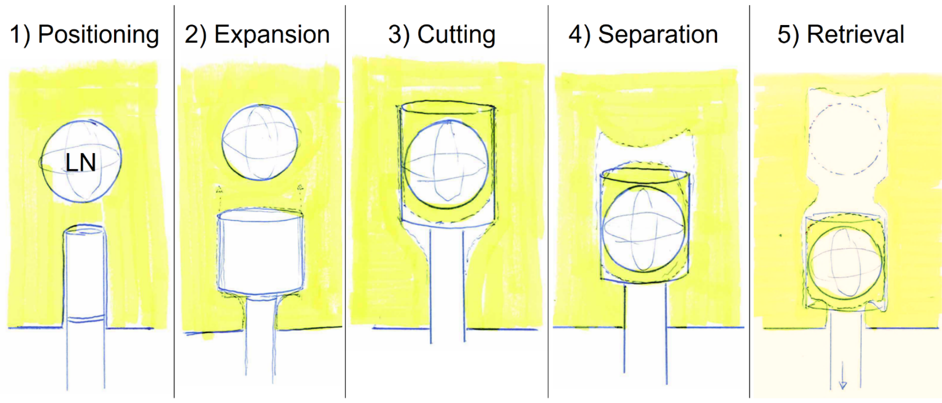

Figure 2.1: General procedure steps of the concept using local expansion. Step 1: Positioning of device in line with target LN. Step 2: Local expansion of cutting ring in front of LN. Step 3: Cutting free the LN from surrounding tissue by forward movement of device over the target. Step 4: Separation of far end to fully disconnect LN from surrounding tissue. Step 5: Retrieval of the LN together with the device

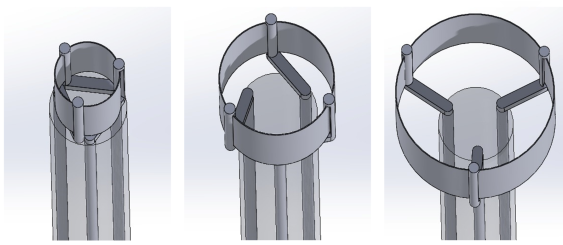

Figure 2.2: Example of possible rod setup to support and actuate local expansion. Clockwise rotation of all rods will cause the connected cutting ring to reshape from a folded position (left) to an expanded position (right)

To position the device, a protective casing is required to protect against tissue damage caused by the cutting ring. Once in position, the protective casing can be removed, allowing for device expansion. Expansion of the device is dependent on the size of the target SLN. The expansion is achieved with the rotation of a number of support rods located in the main shaft of the device. As seen in figure 2.2, rotation of the rods cause an L-shaped hook attached to the far end of the rod to deviate outwards. The hooks support and guide a coiled blade to form an expanding cylindrical cutting ring. The expanded blade can now be used as a cutting tool which is advanced over the target SLN, cutting it free from surrounding tissue. The rods can be actuated through the shaft, ensuring minimal incision size is maintained. During step *4) Separation*, the entire SLN along with a portion excess tissue is disconnected from the surrounding tissue. Once disconnected, the device can now be retrieved while harvesting the SLN. Dependent on the design direction, a suitable separation strategy needs to be selected. Potentially by employing methods such as twisting and tearing the LN, cutting it by closing a thin wire loop or utilising a bipolar or monopolar cutting technique. During step *5) Retrieval*, precautions should be taken to prevent the cutting ring from damaging surrounding tissue during its backward motion. Slight contraction of the ring could serve to both secure the lymph node and decrease the surface area of the device during this step.

2.2.2. Concept - Wire cutter

The wire cutter concept is focused on minimising the incision size and impact on surrounding tissue during and after the operation. This concept is based around the use of a highly flexible material like Nitinol [18]. The five procedural steps are explained below, an overview can be found in figure 2.3.

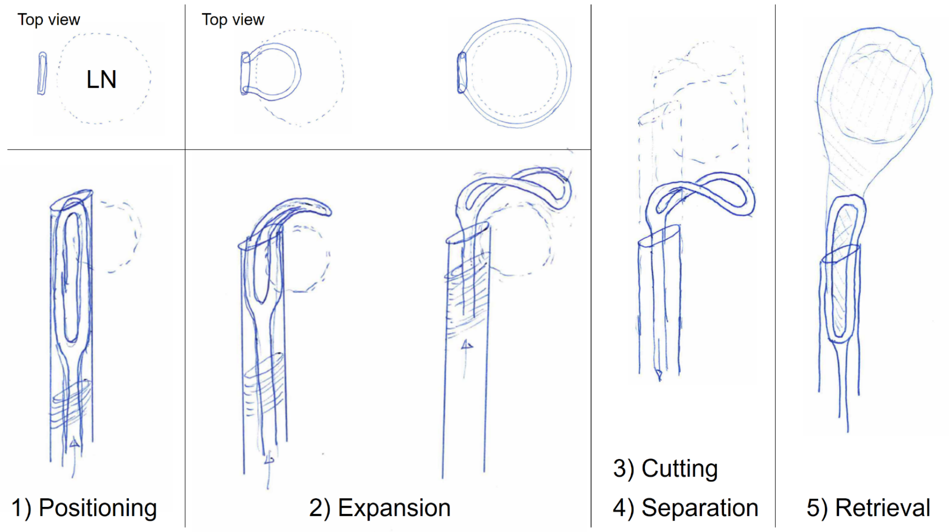

Figure 2.3: General procedure steps of the wire cutter concept. Step 1: Positioning of device next to target LN. Step 2: Expansion of wire by sliding inner tube upwards, wire returns to predetermined shape above LN. Step 3: Slide entire device back to cut area around the LN. Step 4: Retraction of wire back into device will fully separate LN. Step 5: Mesh attached to wire will now surround the LN so it can be retrieved together with the device.

A ring shaped wire restrained by a sleeve will be positioned next to the target SLN as can be seen in figure 2.3. When in position, the wire will be advanced forwards, out of the retaining sleeve, allowing it to return to its original shape partly due to the highly flexible material property. The natural shape of the wire forms an arch above the target SLN when viewed from the side. When looked at from above, a circular profile will surround the entire SLN when the wire is fully extended. This circular profile can now perform a cylindrical cut around the LN when the device is pulled downwards. The cutting procedure is finalised by retracting the wire loop, thereby fully separating the SLN and restoring the device to its minimal profile so it can be retrieved. The separated SLN is harvested by means of a surrounding mesh attached to the wire loop.

This outlines the fundamental concept; however, certain steps may require additional refinement or actions to perform a comprehensive biopsy. Various design aspects, along with their respective advantages and disadvantages are now further analysed.

To make sure the wire will be able to return to its original shape, a flexible material like Nitinol is needed.

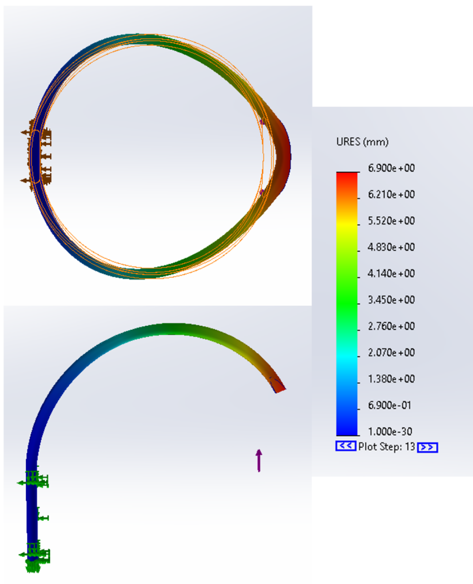

Figure 2.4: Illustration of the result of a FEM-analysis done in Solidworks. It shows the persistence of the circular top view even if the wire is subjected to a cutting force. This illustration was made by simulating a 5N cutting force on the tip of a 22mm diameter circular shaped Nitinol cutting wire. The tip of the 1mm diameter wire is displaced (URES) by almost 7mm while the top view keeps a similar profile.

In addition to its high elastic limit, Nitinol has an unique thermal shape memory property that enhances the reshaping process. If needed, heat can be applied to trigger the shape memory property, which allows the material to remove any plastic deformation if its no longer restrained, this can stimulate the reshape process when the sheath is no longer present. It is the intention that the tissue surrounding the LN provides significantly less resistance compared to a strong metal sheath do make sure the ring can perform the cutting motion without excessive bending. An initial analysis is done using a Nitinol material model in the Solidworks FEM environment to simulate the bending process of the unique ring shape. It demonstrates that when subjected to a cutting force, the circular top view remains intact even after the ring itself is bent.

To allow for the wire to cut though the tissue, a thin wire would be optimal but might not provide the required strength to retain the arc-shape around the SLN. To aid the cutting process, the metal ring can be used as an electrode in a monopolar cutting setup. This can improve the cutting force as well as provide coagulation to stop bleeding during the cut.

As previously noted, attaching a mesh to the ring is needed to enable the extraction of the lymph node from the patient. An alternative approach involves grasping the SLN during positioning and sliding the wire over it while it is held in place by this pinching mechanism.

2.2.3. Concept - Full length expansion

This full length expansion concept is based on insertion techniques for trocars used in laporascopic surgery. It utilises a flexible sheath that is expanded by a wedge-like rod as can be seen in figure 2.5.

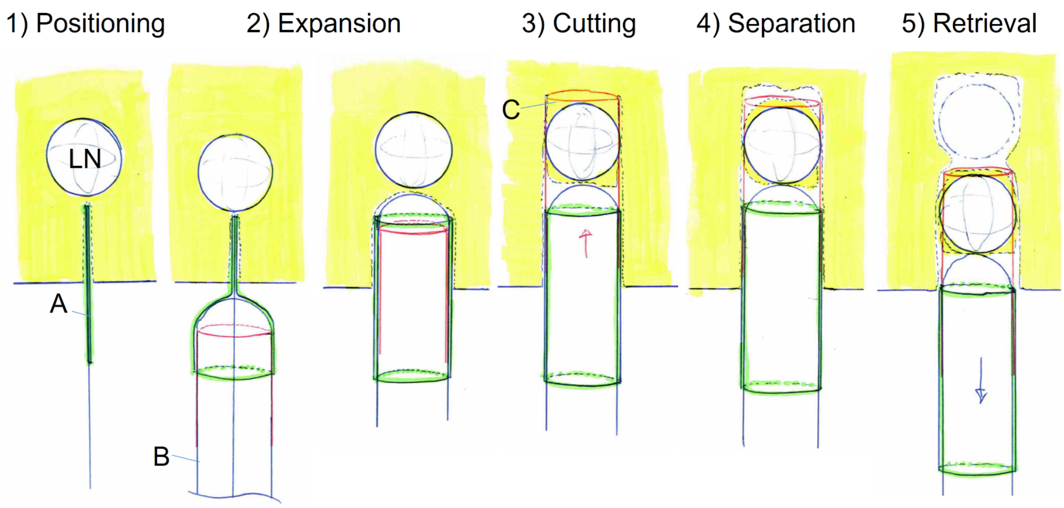

Figure 2.5: General procedure steps of the Full length expansion concept. Step 1: Positioning of sheath (A) in front of the LN by means of a guidance needle. Step 2: Expansion of sheath using wedge (B). Step 3: Separating sides of LN from surrounding tissue by sliding forward a cutting cylinder (C) located around the wedge. Step 4: Fully disconnecting LN from surrounding tissue. Step 5: Retrieval of LN by removing device with LN attached.

The wedge-like rod extends the sheath along its entire length. During this expansion, the skin and surrounding tissue are stretched and displaced. While the skin and tissue experience high disturbance initially, the sheath also serves as a protective layer, preventing any other parts of the device from further interacting with the surrounding tissue. After expansion, the wedge provides a stable guidance for a cutting mechanism to advance over the target SLN. Dependent on medical preference, the cut can be performed using a sharp edge or cauterisation wire. Similar to concept 2.2.1*Local expansion*, a separation step is most likely needed to separate the SLN at the far end of the device. Next to separation with monopolar or bipolar cauterisation, a contracting thin wire loop can be utilised to separate the SLN. Furthermore, such a wire loop can be attached to the tip of several blades; contracting the wire will bend the blades so they can be used to cut free the SLN when the device is rotated. A similar technique can be found in the breast lesion excision system (BLES, Intact Medical, Framingham, USA) [19],[20]. A visualisation of the BLES and potential implementation can be found in figure 2.6. Retrieval of the SLN can now be done by retracting the cutting mechanism and wedge rod containing the SLN. This can be performed with the sheath either attached or left behind. If left behind, it will revert to its original low-profile shape, facilitating removal with reduced tissue damage compared to expanded removal.

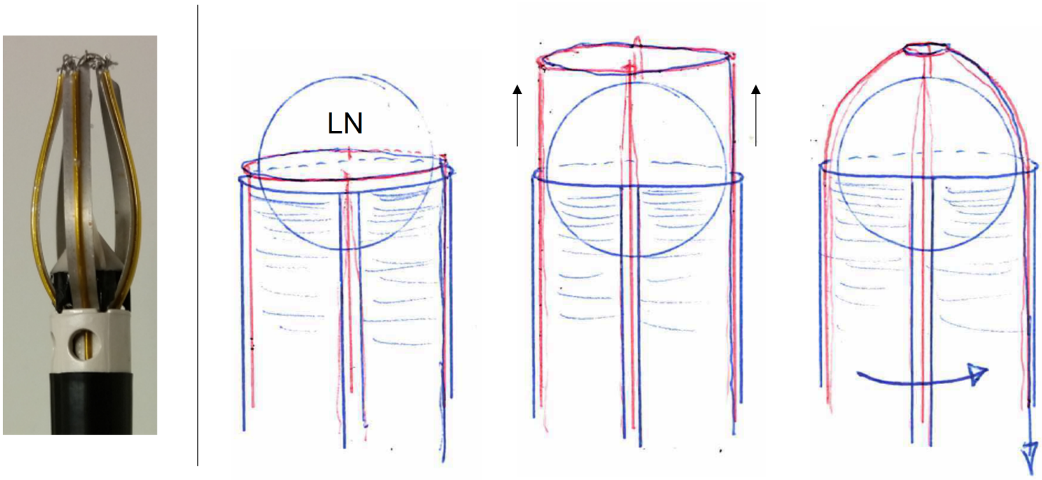

Figure 2.6: Left shows the breast lesion excision system (BLES, Intact Medical, Framingham, USA), on the right the implementation of the BLES during the separation step of the full length expansion concept. The wire and blades are extended from the frame after which the loop is tightened causing the blades to bend inwards. The blades can be used to cut free the SLN when the device is rotated.

2.3. Concept selection

To determine the design direction of this project, each concept is graded based on several selection criteria. For each criteria, the concepts are scored based on expected performance in general and in comparison with the other concepts. A bad expected performance yields 0 points, medium expected performance yields 1 and good expected performance yields 2 points. A total score is determined by adding the weight times its corresponding score for each criteria. Weights are introduced to assign higher priority to certain requirements over others. Weather a criteria has a high priority is decided by the author in consultation with medical and technical professionals. Criteria are created in five categories, each with their own set of subcategories. Invasiveness is defined by the incision size, tissue damage, amount of excess tissue and potential of bleeding infliction. Adaptability of the device is important since variable SLN's are encountered during the procedure. The complexity of the device has an impact on the completion of manufacturing and testing the device within the available project time. It is categorised by the producability, sturdiness, use of active components, procedural steps and user interaction. Safety of the device is categorised by possible fail-safe features and sterilizability. The durability, categorised by reusability and material type, require some forethought but is assumed to be of less importance, resulting in a lower criteria weight. A summary of the concept analysis is provided below, for each concept, the assigned grades can be found in fig 2.7.

Local expansion: When implementing the local expansion concept, the behaviour of the cutting blade must be investigated to ensure proper expansion. One advantage of local expansion is the adaptability to excise different SLN's using a single device while minimising excess tissue. The correct expansion size can be determined while the device is already inserted in the patient. Local expansion permits an incision size smaller than the SLN itself, reducing the impact on the skin. However, this can introduce additional complexity when the device is retrieved in expanded configuration. Additionally, the rods must strike balance; they must be small enough to achieve the desired expansion, yet strong enough to support the blade and facilitate expansion while displacing surrounding tissue.

Wire cutter: The wire cutter concept allows for the smallest footprint of the entire procedure, interacting with minimal surrounding tissue and skin. To further develop this concept however, additional research is required regarding the optimal ring size, shape and material. The ring needs to be able to retract inside the sheath, but also maintain enough resistance inside the axillary tissue during the cutting procedure. A smaller diameter wire or viability of implementing a monopolar cutting tool can greatly decrease the needed cutting force. However, an active wire might cause damage to surrounding tissue due to the fact that the tissue is not pulled aside as is the case in regular monopolar cutting procedures. When dealing with differently sized SLN's, this device can not adapt to minimise excess tissue. Differently sized devices could be created and SLN size and corresponding device size would have to be determined before the procedure.

Full length expansion: When implementing the full length expansion concept, design and construction of the sheath needs the most attention. Stent like structures or a flexible trocar sheath could be used for initial testing to speed up the process [21], [22], [23], [24]. A big advantage of this concept is its simplicity for both the procedure as well as design. The device should be sturdy and safe for the patient and allows for individual disinfection of parts since they can be taken apart. However, a relatively extensive expansion of the skin area is needed, which can be more challenging to achieve compared to the fatty axillary tissue. Design and construction of the sheath needs further research but inspiration can be taken from expandable trocar systems as mentioned. Lastly, similar to the wire cutter concept 2.2.2, this device is not adaptable for variable sized SLN's, a smaller SLN could lead to a lot of excess tissue after extraction. Different scaled versions of the same device might once again solve this issue, but adaptation while inserted inside the patient is still not possible.

For the different concept, grades are assigned to each criteria. The local expansion concept 2.2.1 featuring rotating rods achieves the highest score. While the wire shows better performance when looking at the invasive category, other factors such as the adaptability and complexity show that the local expansion concept is the most promising overall. This design will now undergo further development to progress towards achieving a fully functional MISLNBD.

Criteria	Weight	Local expansion	Wire Cutter	Full length expansion
Invasiveness	35			
Incision size	10	2	2	0
Surrounding tissue damage	10	0	2	1
Excess tissue	10	1	1	0
Bleeding caused	5	1	2	2
Adaptability	15			
One device for different LN sizes	15	2	0	0
Complexity	25			
Producibitlity	6	1	0	2
Strudiness	5	1	0	2
No use of active components	5	2	0	2
Procedure steps	5	2	2	1
User interaction	4	2	2	1
Safety	10			
Fail-safe features	5	1	1	2
Difficult to sterilize	5	1	2	2
Durability	6			
Reusability	3	2	1	2
Material type	3	2	1	1
Total weighted score		126	99	90

Figure 2.7: Decision matrix, allowing for concept comparison using the different selection criteria seen on the left. For each criteria the different concepts are graded. A bad expected performance yields 0 points, medium yields 1 and good yields 2 points. Total weighted scores can be seen at the bottom of the matrix.

3

Design

The next step in the development process, is to take the selected concept and realise a design which can be used to create a proof of concept. Different aspects of the design used during the testing phase will be presented below. Technical drawings of all parts used during testing can be found in appendix D.

3.1. Rods

As can be seen in the concept presentation 2.2.1, the local expansion design uses a main frame that houses a number of rotating rods. An L-shaped hook is located at the end of each rod that will guide and support the expanding blade. The number of rods employed in the design influences several different variables; The amount of supporting points for the cutting ring, the required space inside the main shaft, the expansion factor of the blade and the applied moment on each rod during expansion. When assuming a maximal expansion diameter of 22mm (see section 2.1), the incision size can be estimated using the maximal expansion factor the rods can realise. An estimation is made with 1.5mm rods, for a different number of rods the expansion factor and incision size are shown in table 3.1.

Number of rods	Min. insertion diameter (d)	Expansion factor
2 rods	9 mm	x 2.4
3 rods	10.5 mm	x 2.1
4 rods	12 mm	X 1.8
5 rods	14 mm	X 1.55

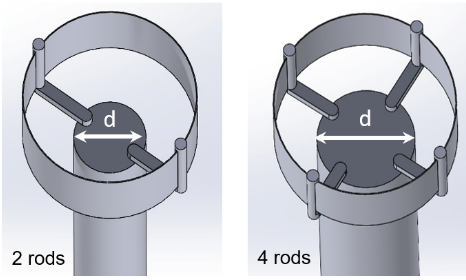

Figure 3.1: Table with the effect of rod number on minimal insertion diameter (d) and expansion factor. Geometric calculation done for maximum expansion of 22 mm and 1,5 mm rod diameter. Examples for 2 and 4 rods are illustrated on the right, highlighting the increase in diameter (d).

Three rods are chosen to create a stable framework to house the cutting ring while the minimal insertion diameter is kept relatively small. The rotating rods are further developed in SolidWorks, keeping in mind fabrication methods and available materials. A circular rod with the desired hook can present challenges during manufacturing. Therefore, angular rods are formed with a single extrusion so they can be created using a laser cutter or with electrical discharge machining (EDM). The resulting design is illustrated in figure 3.2.

To increase the expansion factor, a stepped shape forms the base of the hooks. This allows the hooks to overlap each other when the device is fully closed. To increase the strength of the hooks, the amount of material is optimised through the implementation of two 60-degree bevelled edges. This way the three interlocking hooks fit closely against each other as can be seen in figure **??**.

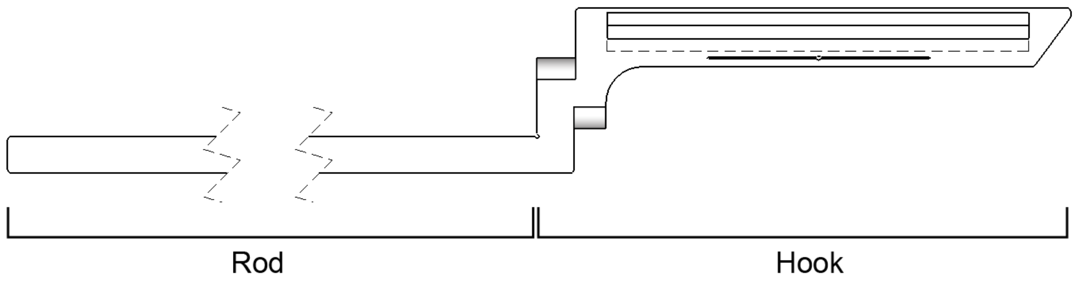

Figure 3.2: Illustration of rotating rod and hook. The rod will go through the main shaft and the hook will house and attach to the the cutting blade. The rod and hook are connected to each other forming a single part. Three rods and connected hooks will be used in the device.

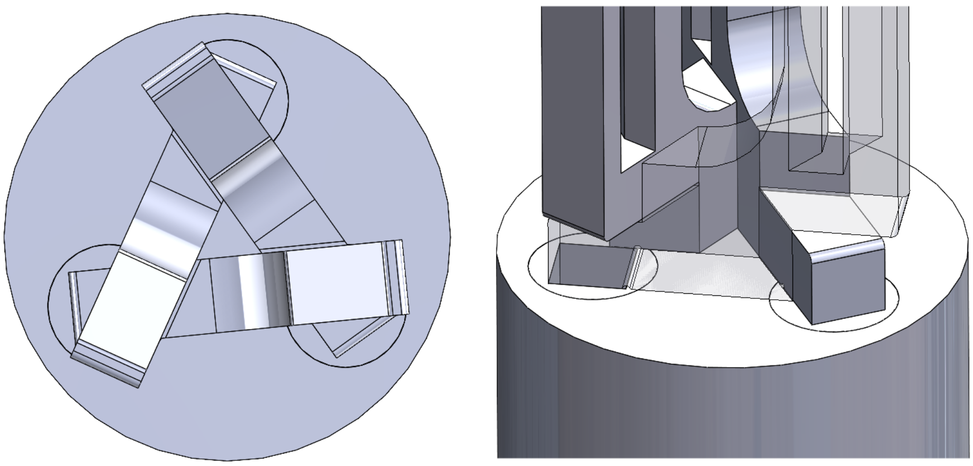

Figure 3.3: Illustration of the rods and connected hooks in closed configuration, the rods are located inside the main shaft. Due to the stepped base and the bevelled edges, the three hooks closely fit each other. This increases the expansion factor and optimises material in the base of the hook to increase its torsional resistance.

Due to the available sheet metal and to introduce a safety factor, size of the rods and hooks is determined to be a square with sides of 2mm.

The integrity of the hooks with these dimensions is verified in section 3.4 using FEM software available in the SolidWorks package of the TUDelft. A technical drawing with all dimensions used for testing can be found in appendix D.

3.2. Main shaft

The main shaft acts as support and guidance for the three rods, its diameter will determine the incision size needed for the procedure. Due to the availability of electrical discharge machining (EDM), the shaft can be made out of a solid cylinder with 3 circular holes. EDM allows for a precision cut hole through the entire length of the shaft. Each rod is supported with two plain bearings located in a counter bore, a widened section at both top and bottom of the shaft as can be seen in figure 3.4. The main shaft has a diameter of 12mm to maintain enough material between the bearings and the shafts outer edge to prevent potential material failure.

The length of the shaft influences the torsional deflection experienced by the rods due to the force needed to push away the surrounding tissue and expand the cutting ring during expansion. A shorter rod length will decrease the deflection, the length however is limited by the depth of the SLN. Its estimated that the average SLN depth is 43 mm [17], the shaft length used in this initial design is 50mm.

The base of the hooks prevent axial movement of the rods further inside the main shaft. To prevent movement in the other direction, rod collars are located at the end of the rods. A counter screw prevents the collar from moving which in its turn blocks lateral movement of the rods and hooks.

For the prototype used in testing; the rods, bearings, and main shaft are manufactured from stain-

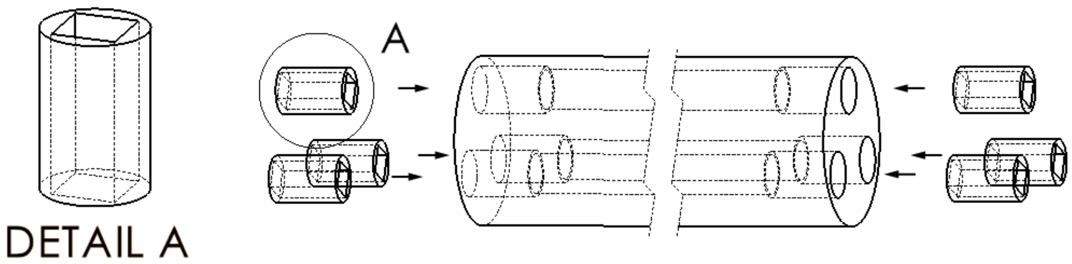

Figure 3.4: Illustration of the main shaft, six bearings fit the counter bores located at both ends of the shaft. The square rods will fit these bearings, containing them while allowing rotation.

less steel due to its availability, high yield strength, durability and corrosion resistance. This will fully represent the medical grade stainless steel that should be used in the final design. Medical grade stainless steel will show similar yield strength but meet the higher corrosion resistance and bio-compatibility standards. Next to this, stainless steel allows for sterilisation of the device prior to the procedure with negligible damage to the material.

3.3. Cutting blade

The cutting blade is made from leaf spring steel due to its elasticity, high yield strength and fatigue resistance. Although not used for testing, medical grade leaf spring steel can be sterilised and used bio-compatibly. The blade is designed to naturally form the smallest diameter of 8.3mm, during expansion it is uncoiled by the hooks that push outwards on the blades inner layer. The shape of the blade before and after expansion can be seen in figure 3.5.

The length needed for the blade to reach full expansion is $pi * 22$mm $= 69$mm, extra length creates an overlapping area to keep the blade in place and prevent it from escaping the slits in the hooks. The blade used is 78mm long, creating an overlap of 9mm. Height of the blade is determined by the maximum LN size of 22mm. The study of Preis [14] shows that a blade of 0.05mm will show a good amount of flexibility wile it is less prone to failing compared to a thinner blade. Testing is done with a blade thickness of 0.05mm.

The cutting blade is positioned inside the housing located in the rotating hooks. To prevent high friction, the height of the slit is set at 23mm, slightly exceeding the blade height. An illustration of the blade and its supporting slits located inside the hooks can be found in figure 3.6. As can be seen, in addition to the supporting slits, a blade attachment slit is present. This attachment slit is present in only one of the three hooks and is used to attach the blade to the device. The indented edge of the blade is positioned inside the attachment slit after which it can be slightly bent around the hook to secure the blade to the device. Pilot holes are needed to perform the closed loop cuts with the EDM wire.

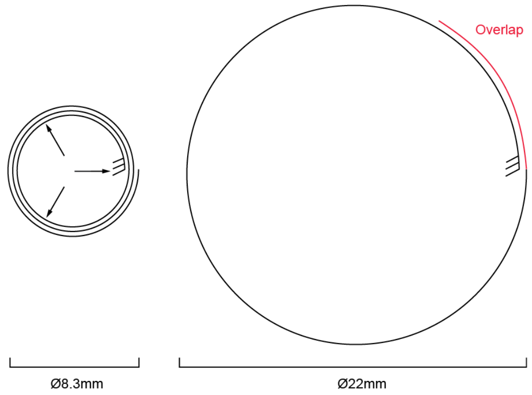

Figure 3.5: Left shows the natural shape of the cutting blade. When hooks are rotated they act as actuation to expand the blade due to forces illustrated by the arrows. When fully expanded (right), the overlap will cause the blade to remain positioned correctly.

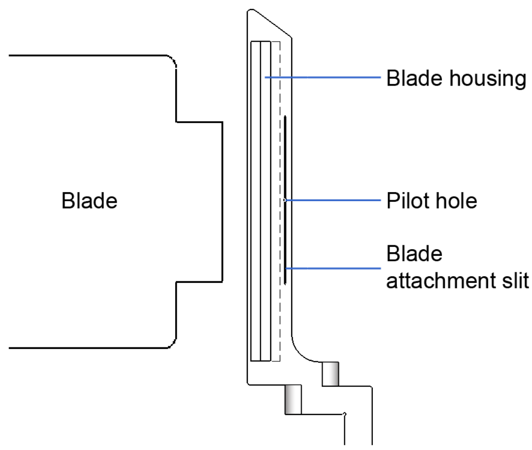

Figure 3.6: Illustration of the partial blade and hook. Location of the blade housing, pilot hole and blade attachment slit are indicated.

3.4. FEM-analysis

The von mises stress and displacement of the hooks are analysed in FEM-software. This analysis is implemented to ensure that the material does not undergo excessive displacement or experience failure during testing. The test was conducted with a force of 5N acting on the slit in the hook, demonstrating that the design effectively withstands such a force. However, since the forces acting on the hook are not yet known, no further shape optimisation is done to decrease the material usage inside the hooks. Results of the FEM-analysis can be found in figure 3.7, a maximal displacement of 0.14mm is observed for the tip of the hook, while stresses remain considerably below the maximum yield stress of 1.742e+08N/m^2

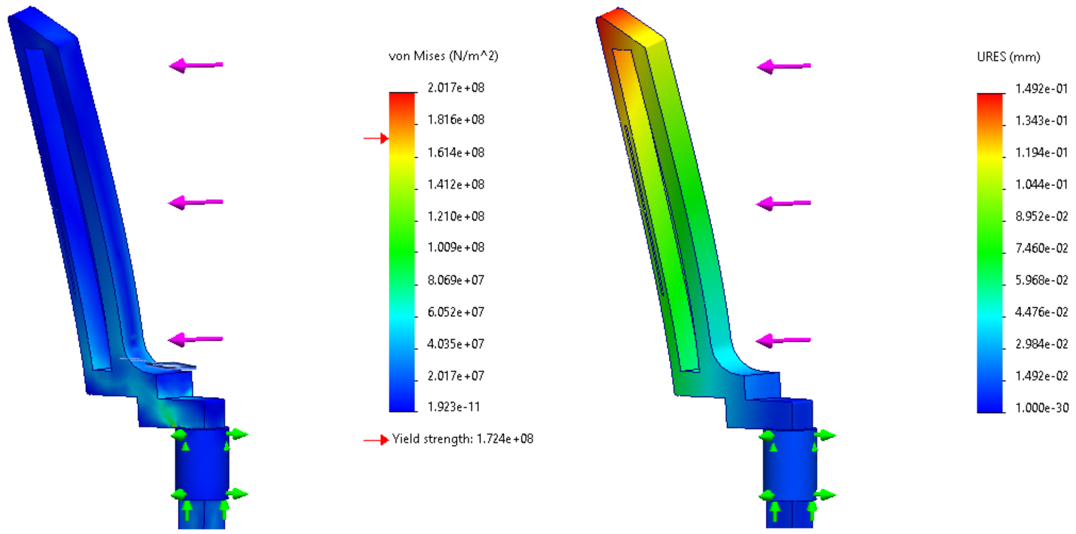

Figure 3.7: FEM-analysis done in Solidworks to analyse a force acting on the stainless steel hooks. A force of 5N applied to the blade housing was analysed. Von Mises stresses can be seen on the left, displacement is illustrated on the right.

3.5. Assembly

Parts are manufactured inside the Dienst Electronische Mechanische Ontwikkeling (DEMO) workshop of the TUDelft. After manufacturing, the following observations are made; The bearings function effectively, facilitating free rotation of the rods, which are securely held in place by the shaft collars. The diameter of the fully expanded blade is 20mm due to the location and size of the slits. The blade size when fully contracted is 8.3mm. Furthermore, it was discovered that the techniques required to create the coiled cutting blade were not readily available. Applied pre-tension is insufficient to achieve the coiled shape of the blade, resulting in only partial curvature. Consequently, the blade diameter is approximately 25mm when not inserted into the device. The materials and techniques to heat treat the blade to potentially reach the 8.3mm diameter were not available, which is why it is decided to test the design using the less coiled blade. The blade will now naturally expand however. To prevent the blade from protruding outward during the procedure, the blade attachment is reversed. This means that the outer layers edge of the blade is attached to the hooks instead of the inner layers edge. A modified attachment slit located on the other side of the blade housing is therefore used during the experiments. The blade design used in testing can be found in appendix D.

4

Design testing and analysis

In this chapter, experiments will be presented that are used to analyse the current design. The primary objective of the experiments is to establish weather the ring can be utilised to expand the cutting blade. Tests are also conducted to investigate the cutting potential of the blade and its ability to retract. First, the methods used for a variety of tests is presented followed by the tests results and analysis.

4.1. Methods

Phantom tissue is made to mimic the axillary tissue typically present around the SLN's. The phantom type used and its creation process is described below in section 4.1.1. Furthermore, an actuation method is needed during the experiments, actuation used during testing can be found in the subsequent section 4.1.2. Finally, the different experiments are presented and explained in subsequent sections 4.1.3, 4.1.4, 4.1.5 and 4.1.6. An overview of the different tests can be seen in figure 4.1.

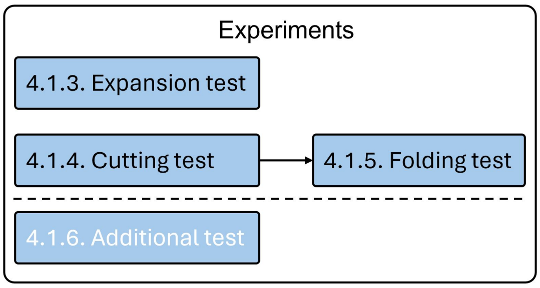

Figure 4.1: Overview of experiments done to analyse the working principles of the current design

4.1.1. Phantom tissue

The phantom tissue is made by mixing and heating gelatin powder and water after which it is poured into plastic containers to stiffen up and be used during testing. For all experiments, four different ratios of gelatin powder to water are utilised to differentiate how firm the gelatin will be. Phantom tissue will not completely mimic the actual axillary tissue, but for this experiment its more important to analyse the influence of a substance uniformly pushing against the sides of the cutting blade. Different gelatin stiffness allows for a step wise build-up of force acting on the device as to not prematurely damage the device during testing. Research shows that a weight percentage of 17,5% gelatin powder to water creates a relatively accurate representation of the axillary tissue [25]. The four percentages used in this research are 5%, 10%, 15%, and 20%. The ratio is calculated using the following formula: *Weight percentage gelatin powder [%] = Weight of gelatin powder [g] / (Weight of gelatin powder [g] + Weight of water [g])*. Appendix A provides information regarding the containers and the methodology to prepare the gelatin for testing.

4.1.2. Actuation

To perform the experiments, an actuation mechanism is created to rotate the hooks as needed to expand or contract the cutting blade. The mechanism controls the rotational movement of the hooks, ensuring they remain in a 120 degree angle relative to each other. Optimally, this is achieved by avoiding interference from experimental results, such as adding frictional forces to the system. An actuation mechanism, illustrated in figure 4.2, is designed in Solidworks and printed with Polylactic Acid (PLA).

Three actuation rods are designed to fit over the square external ends of the rotary rods, similar to the rod collars. A disk with three protrusions is positioned over the shaft of the device. These protrusions, located at 120 deg angles relative to each other, will apply pressure against the actuation rods upon rotation of the disk. Rotation of the disk can be accomplished manually while experiencing minimal friction. A two part holder fits tightly around the main shaft, this allows for the shaft to be manually secured which prevents the device from rotating during the experiment. The holder is tightened with two screws, in addition, double sided tape between the holder and the main shaft prevents the shaft from slipping. The disk is positioned between the rods and the holder, making rotation its only degree of freedom. Technical drawings of all actuation parts are presented in appendix D.

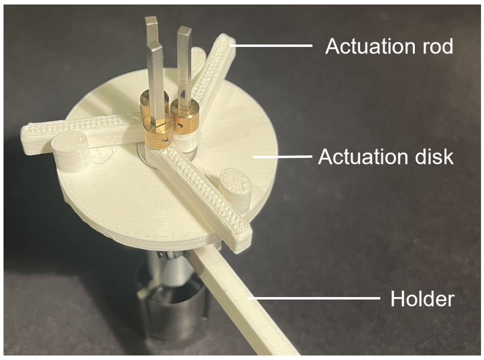

Figure 4.2: Illustration of the actuation mechanism when installed on the device; the rods, disk and holder are indicated.

4.1.3. Expansion test

The expansion test is performed to analyse if the expansion of the cutting blade can be achieved through rotational motion of the three supporting hooks. The experiment is conducted 10 times, twice without tissue and twice in the four different gelatin solutions described in section **??**. To perform the experiment, the tip of the device is positioned in either the air or the phantom material. For the gelatin, a 22 mm deep cylindrical hole is made prior to insertion into which the tip of the device can be positioned. The expansion can now be tested by rotating the three hooks counterclockwise simultaneously. The hooks are actuated using the actuation described in section 4.1.2. To determine the performance of the device during the test, the angle of the hooks is noted, full expansion is reached at 130 degrees of rotation. Next to that, observed deformations or mechanical failures of the device are documented. A detailed procedure and setup of the experiment can be found in appendix B.1. The test results are described in 4.2.1 and documented in appendix C.1.

4.1.4. Cutting test

The purpose of this experiment is to evaluate the cutting blade's ability to cut the gelatin phantom tissue during a forward cutting motion. The test is performed with the device in expanded configuration, meaning that the hooks point outwards from the centre of the device (130 degrees). The device is positioned above the gelatin and manually pushed downward, causing the blade to be pushed into the gelatin. This experiment is conducted 8 times, twice in each of the four different gelatin phantoms. If the blade cuts through the tissue the motion will be continued until the blade reaches a depth of 25mm. To evaluate the device's cutting capabilities, cuts are categorised as either successful or unsuccessful based on if the cutting motion can be completed. Additionally, observations are made during the cutting motion to determine whether this introduces any deformations or mechanical failures. A detailed description of the experimental method and setup can be found in appendix B.2, observations of the full experiment are documented in appendix C.2 and described in the results 4.2.2.

4.1.5. Folding test

This experiment serves as a continuation of the cutting test, aiming to evaluate whether the cutting blade can also be retracted or folded using the same hooks applied for expansion. This retraction can be valuable when aiming to compress or secure the LN during the separation and extraction steps. Similar to the expansion test, this test is conducted 10 times, twice without tissue and twice in the four different gelatin solutions described in section 4.1.1. To perform the experiment, the cutting test must be successfully completed, meaning the cutting blade is now located inside the different gelatin tissue. After this, the hooks are rotated clockwise to obtain a retracting motion. Actuation is carried out using the same actuation disk described in 4.1.2. To evaluate the performance, the shape of the cutting blade and angle of the hooks are noted. The hooks start at a 130 deg angle and are moved to 0 deg to perform a full retraction. Next to this, any other deformation or mechanical failure during the motion is noted. The detailed description of the experimental method and setup can be found in appendix B.3. Observations are described in section 4.2.3 and documented in appendix C.3.

4.1.6. Additional test

Due to the yet to be presented results found for the expansion test of section 4.1.3, an additional test was set up. This test was performed using the exact procedure as the expansion test, however, with a distinct difference in the design of the cutting blade. In this test, the attachment of the cutting blade to the hook of the device is excluded. Meaning that the blade is positioned in the slots of the hooks but is not attached to the hook itself. This is carried out to explore the hypothesis that the current blade attachment negatively affects the expanding motion of the device. Similarly, the angle of the hooks and any deformation or mechanical failures is noted during the experiment. Results of this test are also added to the results of appendix C.4 and described in section 4.2.4.

4.2. Results and analysis

Appendix C shows tables of the results for each test. Observations and findings are documented and if relevant, pictures are included for further clarification. The results and main findings followed by an analysis is now presented for each test.

4.2.1. Expansion test

The results in appendix C.1 show that tests conducted without tissue and in 5% weight percentage gelatin solution allow for full expansion of the blade. Apart from the ring, the device shows no deformation during these tests, in 5% tissue the cutting ring takes on a slight triangular shape around the hooks. For higher density tissues however (10, 15, and 20 weight %), only 10 degrees of rotation is possible. The blade takes on the triangular shape around the hooks after which the motion is blocked. At 15 weight % and 20 weight %, the tip of the hooks also start to show some elastic deformation when rotation is initialised.

Analysis of the results conclude that the blade has a natural tendency to expand due to its dimension of 25mm while outside of the device. This allows for expansion in both air and in 5 weight % tissue. However, inside stiffer tissue natural expansion is prevented and the blade gets pushed inwards against the rotating hooks. Due to the pressure of the hooks and the tight bending of the blade, the frictional forces acting on the blade surface prevent it from moving, an image of the blade is shown in figure 4.3. Further actuation only increase the frictional forces. An illustration of the forces acting on the blade and the hooks can be found in figure 4.4. Since the outer layer of the blade is attached to the hooks, it is thought that removing this attachment will allow the hooks to aid the expansion process, rather than relying on natural expansion of the blade. An additional test was setup to test this hypothesis and can be found in section 4.2.4.

Figure 4.3: Image of the cutting blade that is blocked during expansion

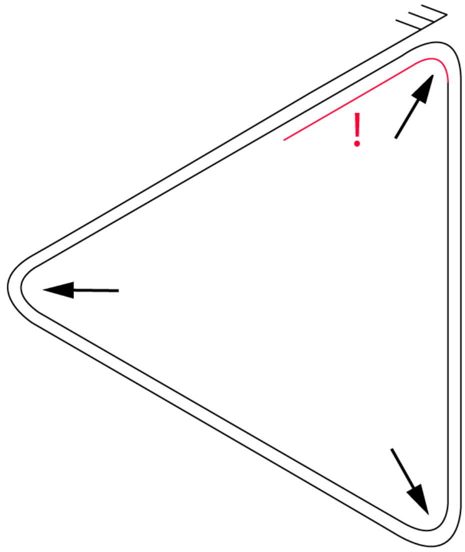

Figure 4.4: Illustration of forces acting on the blade causing for high frictions on the inner blade, blocking the expanding movement

4.2.2. Cutting test

Results of the cutting test documented in appendix C.2, indicate no implications when cutting through lower-density tissues 5, 10 and 15 weight %. As tissue stiffness increases, the cutting motion demands greater effort, to the point where at 20% the the device cant break through the gelatin. Throughout all incisions, the shape of the cutting blade holds up well when exposed to the cutting force needed. The blade gets pushed against the side of the slots inside the hooks but no further deformation of either the blade or the hooks has occurred. The layers of the overlapping part of the ring stay well connected, forming a singular cut inside the phantom tissue.

Analysis of the results show that the ring does not buckle or experience large deformation during any of the cutting tests. The slit is small enough to convey the force of the hooks to the blades front. A sharper blade can potentially further improve the cutting power of the device. Rotation of the entire device does not currently improve the cutting capabilities, presumably due to the relatively large hook endpoints extending beyond the cutting surface. The hooks prevent rotation of the device during the forwards cutting motion. Due to the gelatin shearing, the cutting process requires less effort after the initial insertion. It is difficult to accurately represent the axillary tissue using gelatin, however it can be observed that the current blade can project substantial forward cutting force.

4.2.3. Folding test

The folding tests show that backwards rotation of the hooks is possible, the applied force on the blade however does not cause it to coil up. The hooks bend the blade forming a flattened circular shape as can be seen in figure 4.5. This is true in air but also during tests inside the different stiffness gelatin. To prevent any plastic deformation of the cutting blade, rotation of the hooks is not actuated past the halfway retraction point of 65 degrees. No deformation other than the blade is observed.

The angle in the slits of the hooks allow for the blade to be off-centered. Rotation of the hooks cause the off centered blade to get flattened. All tests inside the tissue show identical results, the force of the tissue to push the blade inwards is not enough to overcome this issue.

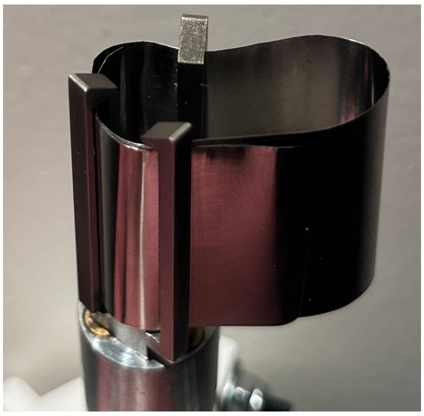

Figure 4.5: Blade during folding test, hooks cause blade to form a flattened cylinder.

4.2.4. Additional test

The detached blade is held in position by the three hooks, allowing for the test to be executed in identical manner as compared to the original expansion test. Although rotation of the blade is possible, testing the blade expansion in air indicates that the blade is also kept in place at full expansion without any tissue surrounding it. In table C.4 similar results can be seen for expansion in air and in 5 weight %. This time however, during 10 weight % percentage or higher, the blade is allowed to expand due to the detached outer layer. Expansion takes more effort for higher density tissues but can be overcome by the force of the hooks aiding the expansion of the blade. Expansion is accomplished for all tissue samples. During the test with highest stiffness of 20 weight % gelatin, the tips of the hooks show slight deflection during the expansion motion. However, while expanding dependent on the rotation of the loose blade, the outer layer of the blade will sometimes extend outwards from the circular blade as can be seen in figure 4.6

The hypothesis that the blade attachment was preventing expansion is confirmed with this test. The outside layer of the blade can now move which allows expansion of the blade without locking the mechanism. However, due to the blades natural tendency to expand, the outer layer of the blade extends from the coil, potentially causing extra damage to surrounding tissue.

Figure 4.6: Image of blade inside device during the additional test, edge of blade extends from coil based on orientation of the blade inside the hooks due to natural tendency to expand.

5
Further design

Moving forward, tree main findings are concluded from the tests executed in the previous chapter 4. These findings can be used to guide the further design of the MISLNBD, considerations for this design can be found in the following section.

5.1. Local expansion

Firstly, expansion can not be achieved with the current blade setup. However, the additional test demonstrates that the hooks apply sufficient outwards force to actuate the cutting blade and displace surrounding tissue. It is demonstrated that blockading issues of the blade can be addressed when the blade is disconnected from the hooks. Considering that a loose blade is not optimal, alternative options must be explored to address this blockading issue. Tests could be conducted using the initial blade design 3.3 which is naturally coiled to 8.3mm and connected to the hooks at the inside edge of the blade. However, a new blade or blade attachment would need to be developed. When the blade is attached differently, the overall design of the cutting blade has high potential to be used in further development of the MISLNBD. To prevent the edge of the blade from extending out from the coiled surface of the edge of the blade, heat treatment might be used to shape the blade to the desired coiled diameter. Even though the hooks will need to overcome the extra force needed to open the leave spring, removing the attachment highly decreased the force needed for expansion. Reduction of friction between the cutting blade layers by lubrication or material removal might also decrease the expansion force needed. However, material removal might decrease the structural stability needed during cutting.

5.2. Cutting motion

The second main finding is concluded from the cutting test 4.2.2. The current blade setup shows great potential to make a surrounding cut with adaptable size around a SLN up to 22mm. To increase the cutting potential, further research into the effect of a sharpened blade edge is essential to decrease the actuation force needed and reduce the pressure on surrounding tissue. Additionally, research into the implications of a monopolar cutting edge can be valuable to increase the cutting capabilities and implement the ability to cauterise tissue in order to reduce the bleeding caused by the device. Adding active components however, does increase the medical classification of the device according to the European union medical device regulation (MDR).

5.3. Retraction of blade

Thirdly, the folding test shows that reverse operation of the expansion does not contract the current blade setup. The need for this contraction has to be evaluated when further developing the MISLNBD. It can be argued that a retraction can cause the SLN to be more secure and reduce damage to surrounding tissue during extraction. However, contraction might not be a necessary step during the procedure. Options to still contract the cutting blade can be investigated; A loop or lasso connected to the hooks surrounding the blades can potentially guide the retraction motion. Tightening of the loop can excert a force on the cutting blade to aid its retraction. Furthermore, the natural contraction force present in the initial cutting blade design of section 3.3 might also improve the contracting capabilities.

5.4. Additional considerations

Apart from the test results, there are additional important considerations that should be taken into account when further developing the MISLNBD.

A slightly longer main shaft is advised to increase the reach and operation freedom of the device. The rods show little deflection and are likely not affected by an increased length of the shaft. The hooks also show little deflection during testing, an accurate estimation of the actuation force can be used to optimise the parts dimensions and further decrease the main shaft diameter and therefore the incision size.

The focus of this thesis was to test the feasibility of a new expansion actuation method. The entire SLNB procedure however, still needs further attention. Insertion techniques are needed like a removable plastic casing to protect surrounding tissue and guide the device during positioning. After expansion and cutting around the SLN, separation techniques should be investigated to fully separate the SLN from surrounding tissue. A lasso connected to the hooks of the blade can potentially be used to perform this separation step. Other options, like monopolar cutting or tearing the tissue might also be viable options. Extraction of the device is now achieved without protection, protective measures like contraction of the cutting blade or a protective flexible casing could be applied to decrease the damage done during removal of the device.

Finally, from an economic point of view, manufacturability of the device can be improved to increase its cost-effectiveness when introduced to the market. Material reduction, reusability options or an efficient supply chain using standard available components can all contribute to possible commercialisation of the MISLNBD.

6 Discussion and Conclusion

Limitations and points of discussion are addressed in the following section followed by the conclusion of the thesis.

6.1. Discussion

There are several points that need consideration regarding this thesis. This project focused on the feasibility of rotating rods as the expansion technique for a MISLNBD. Tests have shown the potential of the technique in step *2) Expansion* and step *3) Cutting* of the SLNB procedure. Although given attention, testing and further development of the other SLNB steps like *1) Positioning, 4) Separation* and *5) Retrieval* is needed to create a fully functional biopsy device. As described in chapter 5 Further design, mainly the SLN collection process needs further attention, focusing on to what extend a separation step is needed and the ability to harvest the SLN after dissection.

Furthermore, although the cutting capability has been tested in gelatin representing the axillary tissue around the SLN's, the exact environment is not simulated by pure gelatin. Connecting lymph ducts, the effect of the dermis and epidermis tissue and structure of the axillary or adipose tissue all influence the ability for the device to be perform a forward cutting motion. Potential improvements of the cutting blade are mentioned, when fully developed, tests on animal tissue and eventually human tissue should be done to confirm findings in this early stage.

Another point of discussion is that this device relies on having sufficient space between the target SLN and the skin layers of the patient. This distance is different in each patient and SLN so the device might not always be suitable. However, this device is designed to function both small and significantly large SLN's. Scaled-down versions of the device designed for a reduced range of SLN sizes can decrease the size of the blade significantly. This will reduce the room needed to position and expand the device while still allowing for an adaptable cutting blade.

6.2. Conclusion

The sentinel lymph node biopsy procedure for melanoma patients can be improved with the use of a minimally invasive sentinel lymph node biopsy device. This thesis shows the early stage designing process of such a device, which can reduce overall tissue damage and opens up possibilities to remove the need for general anaesthesia and therefore the need for an operating room. The design of a device that can locally expand a circular cutting blade is presented. The tests main conclusion is that three rods can indeed be used to actuate variable expansion of such a cutting blade. Subsequently, the blade can be used to cut around different sized target lymph nodes. Furthermore, actuation of this expansion can be achieved through a minimally invasive shaft from outside the patients body. Although further steps of the procedure need to be addressed in order to create a fully functional biopsy device, this thesis shows the potential and feasibility of a locally expanding adaptable cutting blade and provides recommendations for further development steps in the design of a MISLNBD.

References

[1] D. J. Ruiter et al., “Pathologic staging of melanoma.,” *Seminars in oncology*, vol. 29, no. 4, pp. 370–381, 2002. DOI: https://doi.org/10.1053/sonc.2002.34116.

[2] L. E. Davis et al., “Current state of melanoma diagnosis and treatment.,” *Cancer Biol Ther*, vol. 20, no. 11, pp. 1366–1379, 2019. DOI: https://doi.org/10.1080/15384047.2019.1640032.

[3] D. Elder, “Tumor progression, early diagnosis and prognosis of melanoma.,” *Acta Oncol*, vol. 38, no. 5, pp. 535–547, 1999. DOI: https://doi.org/10.1080/028418699431113.

[4] N. U. Dogan et al., “The basics of sentinel lymph node biopsy: Anatomical and pathophysiological considerations and clinical aspects.,” *J Oncol*, vol. 2019, p. 3 415 630, 2019. DOI: https://doi.org/10.1155/2019/3415630.

[5] V. K. Sondak, J. S. Zager, J. L. Messina, and J. M. Thomas, “Sentinel lymph node biopsy as the standard of care for cutaneous melanoma.,” *Clinical advances in hematology & oncology*, vol. 5, no. 6, pp. 483–490, 2007.

[6] E. Z. Keung and J. E. Gershenwald, “The eighth edition american joint committee on cancer (ajcc) melanoma staging system: Implications for melanoma treatment and care.,” *Expert Review of anticancer therapy*, vol. 18, no. 8, pp. 775–784, 2018. DOI: https://doi.org/10.1080/14737140.2018.1489246.

[7] S. L. Wong et al., “Sentinel lymph node biopsy and management of regional lymph nodes in melanoma: American society of clinical oncology and society of surgical oncology clinical practice guideline update,” *Ann Surg Oncol*, vol. 25, no. 2, 2017. DOI: https://doi.org/10.1245/s10434-017-6267-7.

[8] D. E. Branisteanu et al., “Sentinel lymph node biopsy in cutaneous melanoma, a clinical point of view,” *Medicina (Kaunas)*, vol. 58, no. 11, 2022. DOI: https://doi.org/10.3390/medicina58111589.

[9] B. E. Wright et al., “Importance of sentinel lymph node biopsy in patients with thin melanoma.,” *Arch Surg*, vol. 143, no. 9, pp. 892–899, 2008. DOI: https://doi.org/10.1001/archsurg.143.9.892.

[10] V. M. Moncayo, J. N. Aarsvold, and N. P. Alazraki, “Lymphoscintigraphy and sentinel nodes.,” *Journal of nuclear medicine*, vol. 56, no. 6, pp. 901–907, 2015. DOI: https://doi.org/10.2967/jnumed.114.141432.

[11] R. Essner, “Surgical treatment of malignant melanoma.,” *Surg Clin North Am*, vol. 83, no. 1, pp. 109–156, 2003. DOI: https://doi.org/10.1016/S0039-6109(02)00205-0.

[12] P. C. N. et al., *Lymphedema, Complete Medical and Surgical Management*, 1st ed. Stuttgart: CRC Press, Taylor and Francis Group, 2016, ISBN: 9781626236714.

[13] M. I. Joosen, “Minimally invasive sentinel lymph node biopsy,” Master thesis, Delft University of Technology, Delft, Netherlands, Jan. 2021.

[14] L. R. Preis, “Minimally invasive sentinel lymph node biopsy: From surgery to outpatient procedure,” Master thesis, Delft University of Technology, Delft, Netherlands, Jun. 2022.

[15] A. J. Mommersteeg, “Literature review on structure and actuation of existing expandable rings to be used in the design of a minimal invasive sentinel lymph node biopsy device,” Master literature review, Delft University of Technology, Delft, Netherlands, Oct. 2021.

[16] M. D. Justin Merkow et al., “Association of sentinel lymph node diameter with melanoma metastasis,” *The American Journal of Surgery*, vol. 212, no. 2, pp. 315–320, 2016, ISSN: 0002-9610. DOI: https://doi.org/10.1016/j.amjsurg.2015.09.022. [Online]. Available: https://www.sciencedirect.com/science/article/pii/S0002961016300113.

[17] G. C. Bentel et al., “Variability of the depth of supraclavicular and axillary lymph nodes in patients with breast cancer: Is a posterior axillary boost field necessary?” *Int J Radiat Oncol Biol Phys*, vol. 47, no. 3, pp. 755–8, 2000. DOI: https://doi.org/10.1016/S0360-3016(00)00485-5.

[18] D. Kapoor, “Nitinol for medical applications: A brief introduction to the properties and processing of nickel titanium shape memory alloys and their use in stents,” *Johnson Matthey Technology Review*, vol. 61, no. 1, pp. 66–76, 2017. DOI: https://doi.org/10.1595/205651317X694524.

[19] S. D. Allen, A. Nerurkar, and G. U. Della Rovere, “The breast lesion excision system (bles): A novel technique in the diagnostic and therapeutic management of small indeterminate breast lesions?” *Eur Radiol*, vol. 21, no. 5, pp. 919–924, 2011. DOI: https://doi.org/10.1007/s00330-010-2000-7.

[20] e. a. Sanderink W. B. G., “A systematic review on the use of the breast lesion excision system in breast disease.,” *Insights into Imaging*, vol. 10, no. 1, p. 49, 2019. DOI: https://doi.org/10.1186/s13244-019-0737-3.

[21] R. Csaba, T. Wanchell, and K. Azarbarzin, “Trocar insertion apparatus,” US 20050203565, Sept. 15, 2005.

[22] S. P. Moenning, “Trocar-cannula complex, cannula and method for delivering fluids during minimally invasive surgery,” WO 2007040866, Okt. 25, 2006.

[23] W. R. Dubrul, R. E. Fulton, and R. M. Curtis, “Tissue removal methods and apparatus,” WO 2000074561, June 5, 2000.

[24] A. J. Mackenzie and J. E. Carlson, “System and method for establishing vascular access,” WO 2002074174, Nov. 28, 2001.

[25] Y. Jheng and C. Lin, “Fabrication and testing of breast tissue-mimicking phantom for needle biopsy cutting – a pilot study,” *2017 Design of Medical Devices Conference*, V001T08A022, 2017. DOI: https://doi.org/10.1115/DMD2017-3505.

[26] Oetker Professional. “Gelatinepoeder.” (2024), [Online]. Available: https://www.oetker-professional.nl/assortiment/bakken/bakingredienten/gelatinepoeder (visited on 08/04/2024).

A

Gelatin phantom preparation

The gelatin used during testing is Dr. Oetker Professional clear gelatin in powder form [26]. Clear plastic containers are used to shape and store the phantoms, the container has a height of 93mm with average diameter of 75mm. Each container can fit around 350g gelatin phantom tissue, the used weights to fill one container are shown in figure A.1.

Weight percentage gelatin powder to water	Weight of gelatin powder	Weight of water	Total weight
5%	17.5g	332.5g	350g
10%	35g	315g	350g
15%	52.5g	297.5g	350g
20%	70g	280g	350g

Figure A.1: Table of gelatin powder and water ratios used for a single container of gelatin phantom tissue.

The following steps show the process of creating the gelatin tissue:

1. Measure out the correct quantities of tab water and gelatin (see Figure A.1), multiple batches can be created at once.
2. Let gelatin soak in 3 times as much water for 10 minutes
3. Break up the soaked gelatin by hand or with a spatula
4. Heat up the residual water in a saucepan before adding the soaked gelatin
5. Continuously stir the mixture until homogeneous, do not let it boil
6. Pour mixture into the containers through a fine mesh sieve
7. Remove foam layer so it does not block the view when gelatin is stiff.
8. Let rest until cooled down to room temperature
9. Once cooled, refrigerate solution for at least 24 hours
10. Prior to testing, remove container from fridge and wait until room temperature is reached

B

Testing methods

This appendix shows steps taken to perform the different experiments done in this thesis.

B.1. Expansion test

Following steps are taken to perform all the expansion tests, the tests are performed identically for the different gelatin types. Results are documented in appendix C figure C.1.

1. Create a hole of 12 mm diameter and 30 mm depth inside the phantom tissue. A pen cap was used during these experiments but anything else can be used as long as it doesn't impact the surrounding tissue.
2. Make sure the device is in its contracted position.
3. Manually position device with contracted cutting ring inside hole in gelatin.
4. Perform expansion by turning actuation disk counterclockwise. Block rotation of the rest of the device using the 3D printed holder attached to the main shaft of the device.
5. Actuation is stopped when hooks are fully expanded (130 deg), the device will automatically block due to the 3D printed rods.
   OR
   Actuation is stopped when its not or no longer possible to manually rotate the actuation disk to perform the expansion or to prevent any clear damaging of the device.

B.2. Cutting test

Following steps are taken to perform all the expansion tests, the tests are performed identically for the different gelatin types. Results are documented in appendix C figure C.2.

1. Make sure the device is in expanded configuration, all hooks point outwards (130 deg from closed position)
2. Position the device above the gelatin surface, make sure that for each new test an intact part of the gelatin is used.
3. Force the device downwards so the cutting ring interacts with the gelatin.
4. Motion is stopped until device reaches a depth of around 25mm.
   OR
   Motion is stopped if the device can not or no longer be manually inserted inside the target tissue or to prevent any clear damaging of the device.

B.3. Folding test

Following steps are taken to perform all the expansion tests, the tests are performed identically for the different gelatin types. Results are documented in appendix C figure C.3.

1. Continuation of test B.2
2. When depth of 25mm is not reached, this test can not be done.
3. When depth of 25mm is reached, the device is held in place with the 3D printed holder.
4. The actuation ring is manually rotated clockwise, performing a closing rotation of the hooks.
5. Rotation is stopped when device is fully closed (hooks reach 0 deg rotation)
   OR
   Rotation is stopped when manual actuation is no longer possible or to prevent any clear damaging of the device.

B.4. Additional test

The additional test follows the same steps as the Expansion test shown in appendix B.1. The difference between the tests is the attachment removal of the blade to the hooks as described in section 4.1.6.

C

Test results

Expansion test*

Weight percentage gelatin powder to water	No tissue	5%	10%	15%	20%
Maximum possible angle of hooks, from 0 deg util a max expansion of 130 deg.	130 deg, Full expansion	130 deg, Full expansion	10 deg, Only very slight rotation possible	10 deg, Only very slight rotation possible	10 deg, Only very slight rotation possible
Observed deformation or mechanical failure of parts of the device	No deformation	Cutting blade is slightly deformed at full expansion taking a more triangular shape. Triangle less present further from shaft.	Cutting blade is deformed into triangular shape. When more force is applied past the maximum possible angle, tip of hooks flex slightly.	Cutting blade is deformed into triangular shape. When more force is applied past the maximum possible angle, tip of hooks flex slightly.	Cutting blade is deformed into triangular shape. When more force is applied past the maximum possible angle, tip of hooks flex slightly.

*For all the test, the single repetition shows similar results

Figure C.1: Expansion test

Cutting test*

Weight percentage gelatin powder to water	5%	10%	15%	20%
Outcome of cutting test	Successful, cuts through tissue easily	Successful, cuts through tissue easily	Successful, difficult to break though initially. Cuts through tissue steadily afterwards.	Unsuccessful, couldn't break through initial gelatin layer. Succeeds cutting through tissue after using sharp object to aid initial cut.
Observed deformation or mechanical failure of parts of the device	Blade gets pushed against side of slit in hook. No further flexion or deformation	Blade gets pushed against side of slit in hook. No further flexion or deformation	Blade gets pushed against side of slit in hook. No further flexion or deformation	Blade gets pushed against side of slit in hook. No further flexion or deformation

*For all the test, the single repetition shows similar results

Figure C.2: Cutting test

Folding test*

Weight percentage gelatin powder to water	No tissue	5%	10%	15%	20%
Maximum possible angle of hooks, starting at 130 deg with full closure at 0 deg.	65 deg, no further rotation to prevent plastic deformation of blade.	65 deg, no further rotation to prevent plastic deformation of blade.	65 deg, no further rotation to prevent plastic deformation of blade.	65 deg, no further rotation to prevent plastic deformation of blade.	65 deg, no further rotation to prevent plastic deformation of blade.
Observed deformation or mechanical failure of parts of the device	Cutting blade is deformed by hooks, taking on the shape of a flattened circle.	Cutting blade is deformed by hooks, taking on the shape of a flattened circle.	Cutting blade is deformed by hooks, taking on the shape of a flattened circle.	Cutting blade is deformed by hooks, taking on the shape of a flattened circle.	Cutting blade is deformed by hooks, taking on the shape of a flattened circle.

*For all the test, the single repetition shows similar results

Figure C.3: Folding test

Additional test*

Weight percentage gelatin powder to water	No tissue	5%	10%	15%	20%
Maximum possible angle of hooks, from 0 deg util a max expansion of 130 deg.	130 deg, full expansion	130 deg, full expansion	130 deg, full expansion	130 deg, full expansion	130 deg, full expansion
Observed deformation or mechanical failure of parts of the device	No deformation, outer layer of blade sticks out during and after expansion	No deformation, outer layer of blade sticks out during and after expansion	No deformation, outer layer of blade sticks out during and after expansion	No deformation, outer layer of blade sticks out during and after expansion, slight deflection of hooks when too much force is applied	No deformation, outer layer of blade sticks out during and after expansion, slight deflection of hooks during expansion

*For all the test, the single repetition shows similar results

Figure C.4: Additional test

D
Technical Drawings

This appendix contains technical drawings of all the parts used in this research. Keep in mind that most of the parts are used using computer controlled machining which allows for automatic recreation of these dimensions.

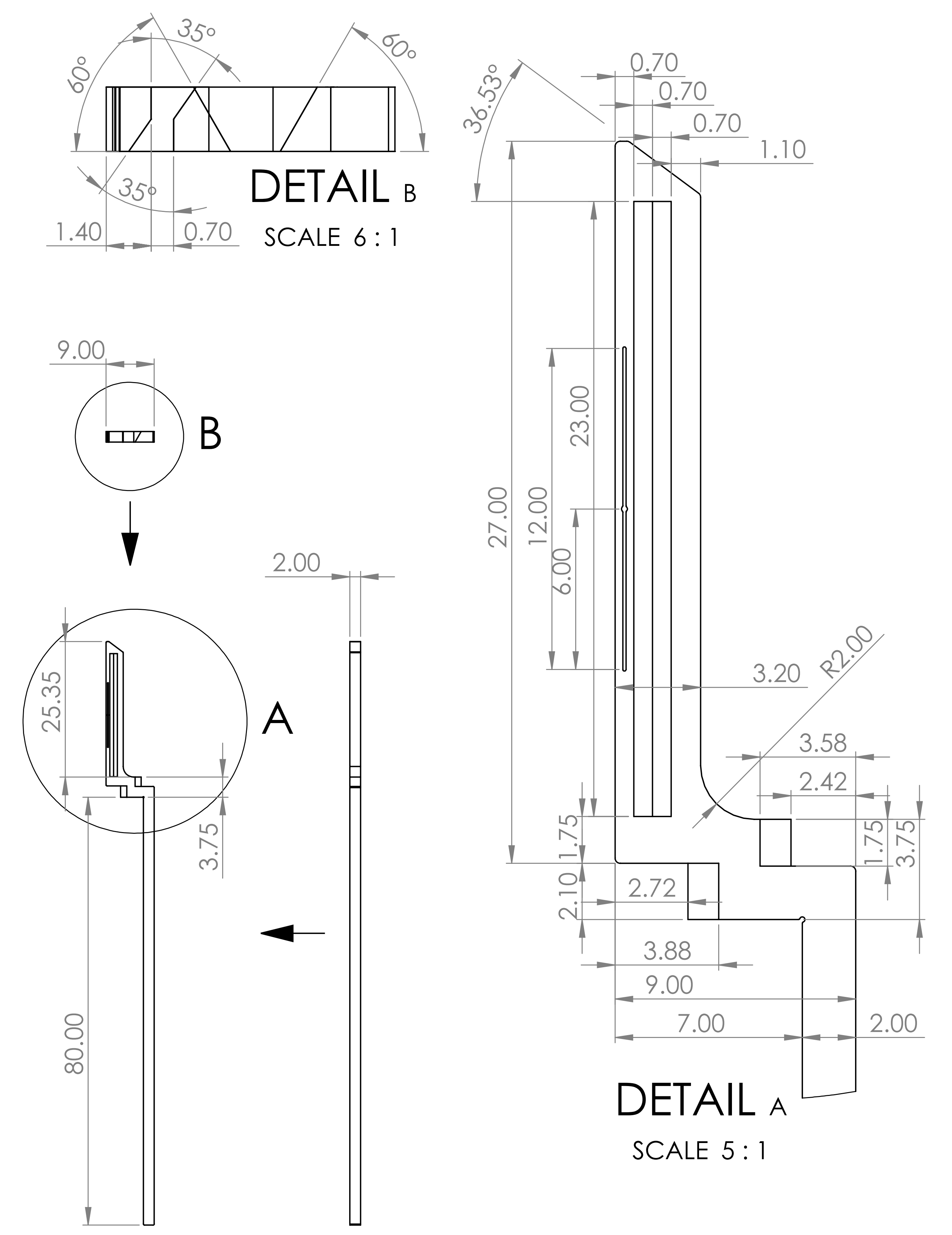

	units mm	scale 1:1	quantity 3	date 09/04/2024	remark Created with EDM wire cutting
material				mass gr	
author A.J.Mommersteeg				group /	TU Delft Delft University of Technology
name **Rod_with_Hook**			format A4	drawing no. 01	

C:\Users\aartm\OneDrive\Desktop\afstuderen\SW\drawings\

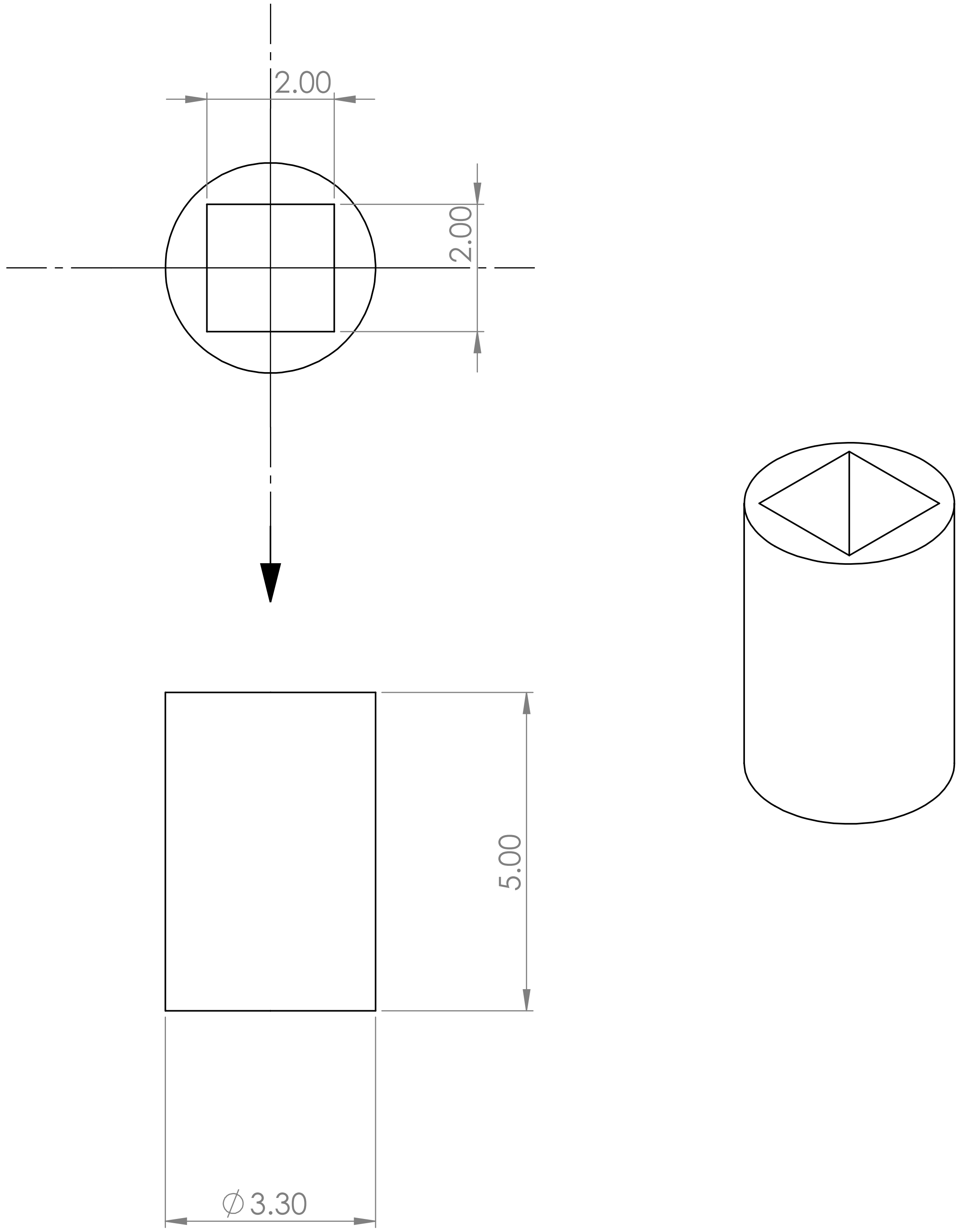

	units mm	scale 10:1	quantity 6	date 09/04/2024	remark /
material				mass gr	
author A.J.Mommersteeg				group /	TU Delft Delft University of Technology
name **Lager**				format A4	drawing no. 02

C:\Users\aartm\OneDrive\Desktop\afstuderen\SW\drawings\

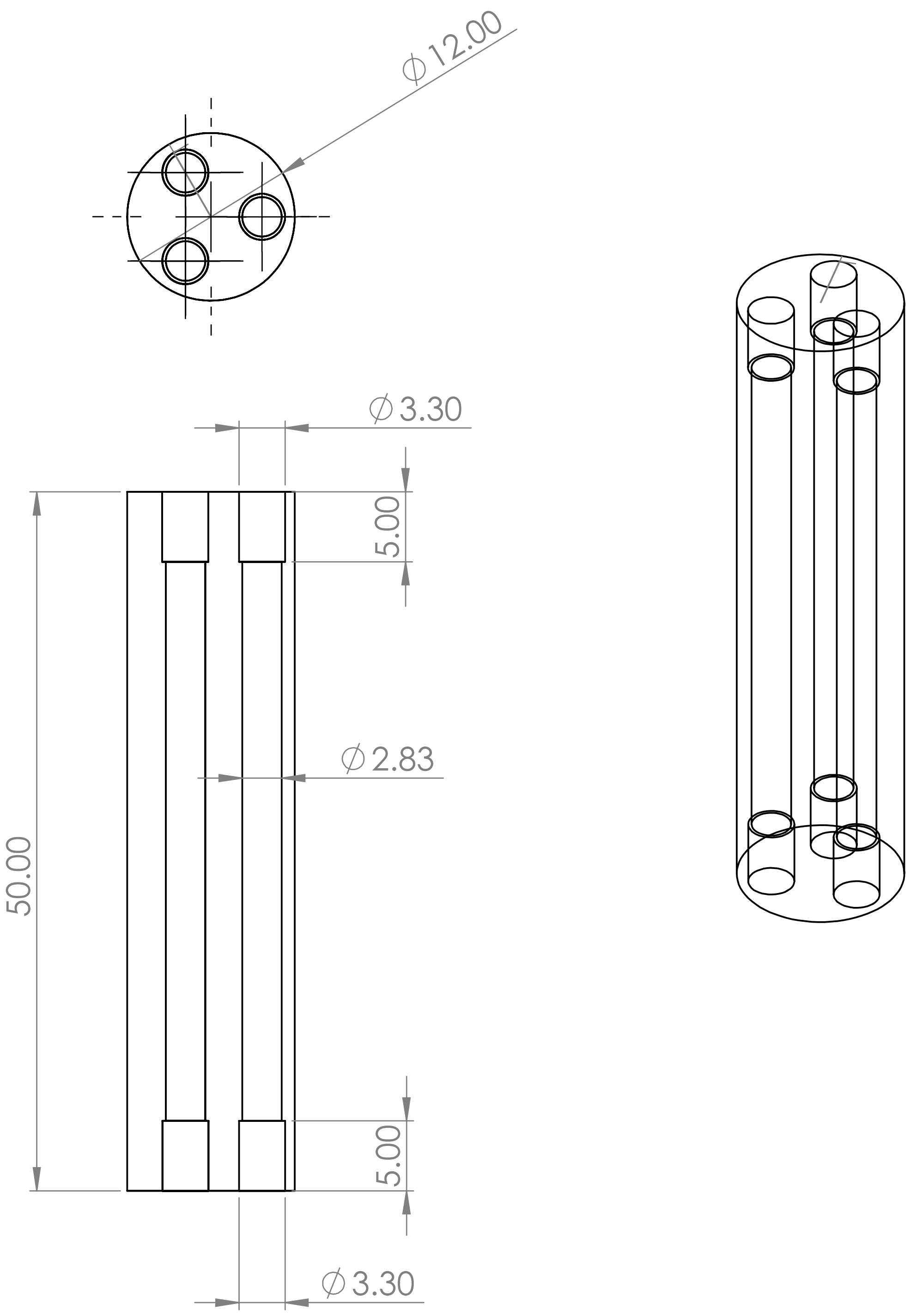

3 Holes, identical dimensions

units mm	scale 2:1	quantity 1	date 09/04/2024	remark /
material			mass gr	TU Delft — Delft University of Technology
author A.J.Mommersteeg			group /	
name **Base**			format A4	drawing no. 03

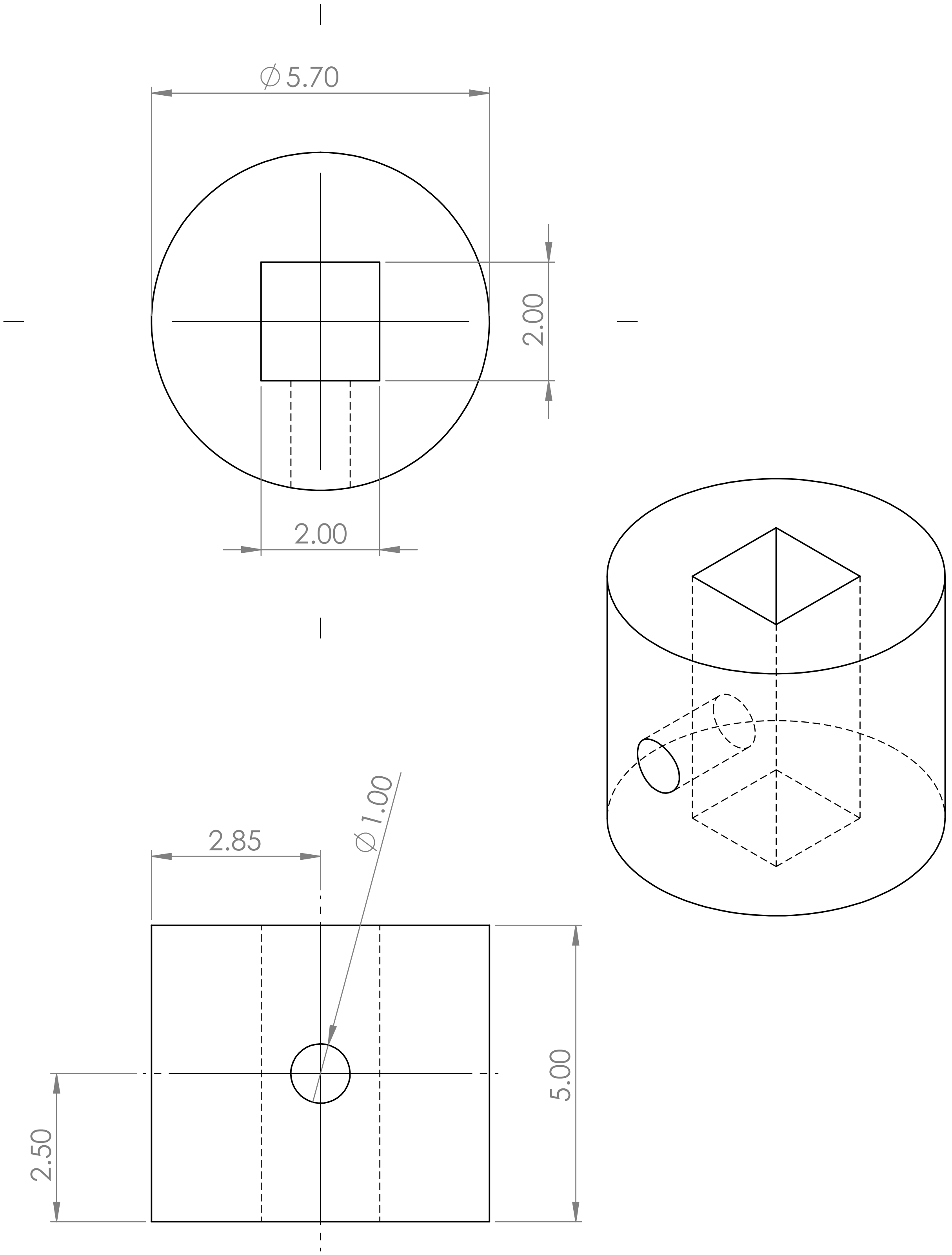

units	scale	quantity	date	remark
mm	10:1	3	10/04/2024	/

material	
mass	gr
author	A.J.Mommersteeg
group	/

TU Delft – Delft University of Technology

name	format	drawing no.
ShaftCollar	A4	04

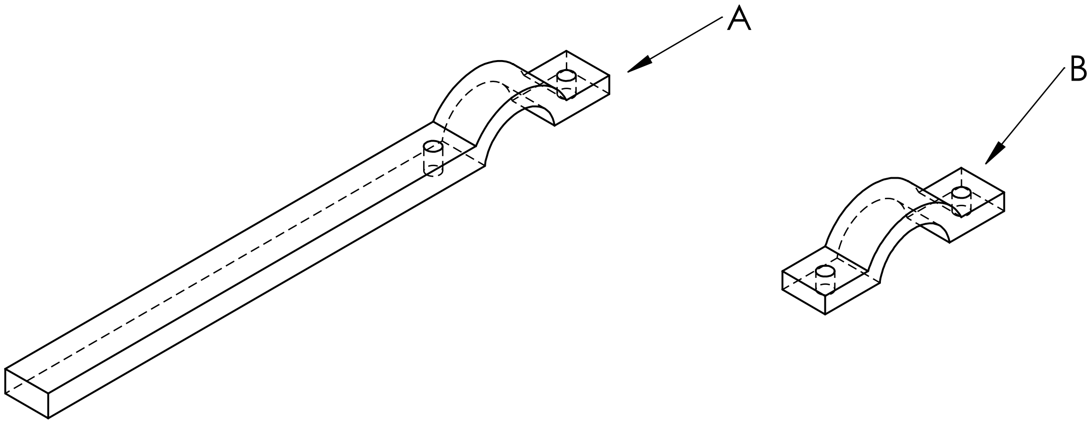

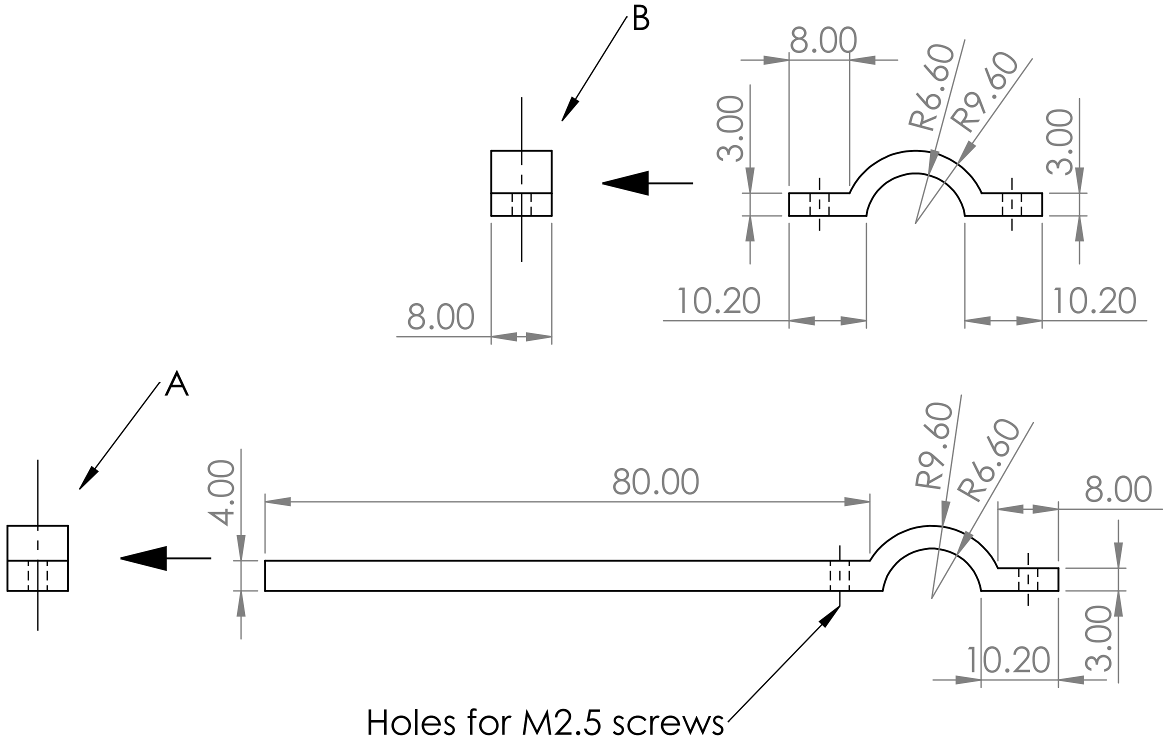

	units mm	scale 1:1	quantity 1	date 10/04/2024	remark /
material				mass gr	TU Delft Delft University of Technology
author A.J.Mommersteeg				group /	
name Holder and Holder lid				format A4	drawing no. 05

C:\Users\aartm\OneDrive\Desktop\afstuderen\SW\drawings\

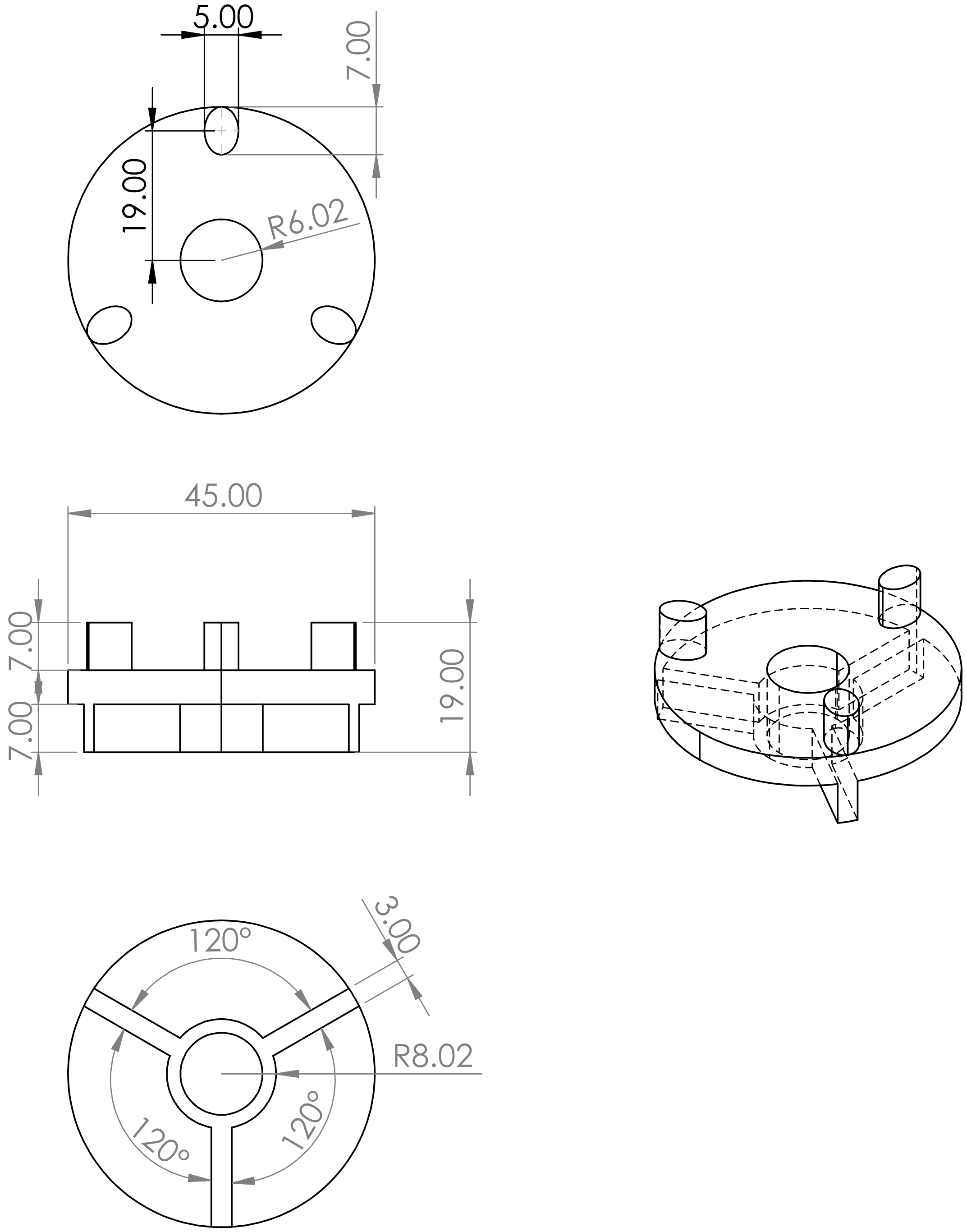

units	scale	quantity	date	remark
mm	1:1	1	10/04/2024	/

material

mass gr

author A.J.Mommersteeg

group /

TU Delft Delft University of Technology

name **Disk**

C:\Users\aartm\OneDrive\Desktop\afstuderen\SW\drawings\

format A4

drawing no. 06

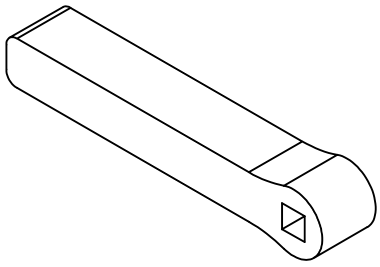

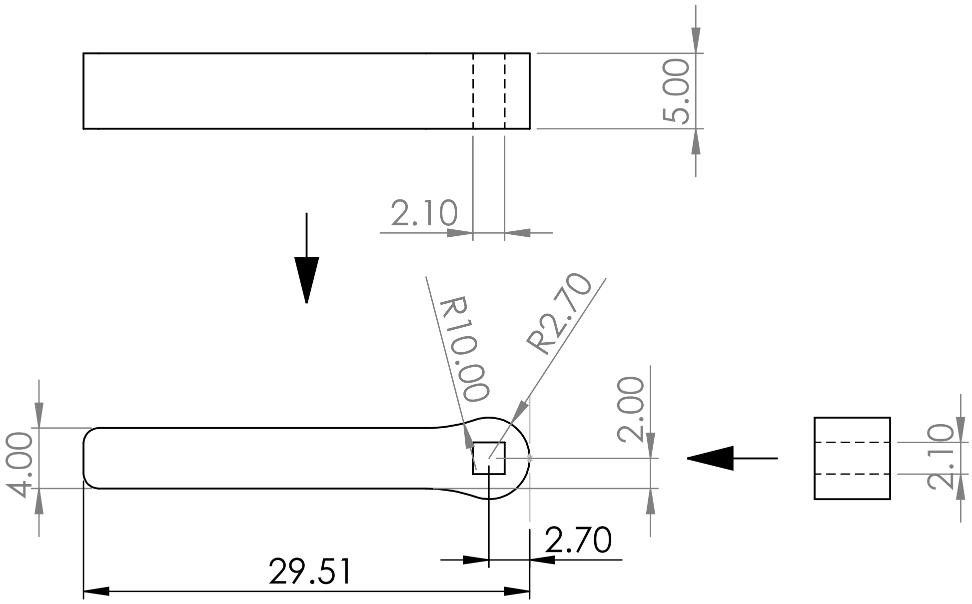

	units mm	scale 2:1	quantity 3	date 10/04/2024	remark /
material				mass gr	Delft University of Technology
author A.J.Mommersteeg				group /	
name ActuationRod				format A4	drawing no. 007

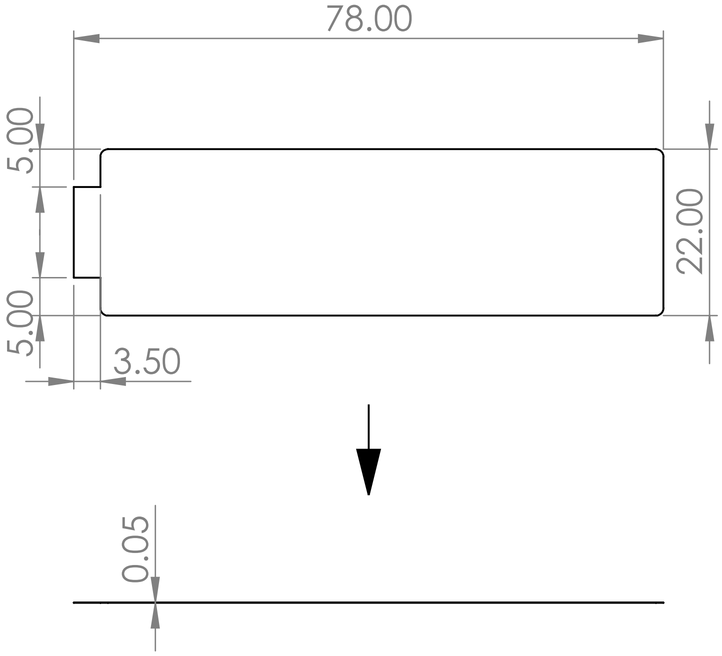

	units	scale	quantity	date	remark
	mm	1:1	1	11/04/2024	/
material				mass gr	TU Delft Delft University of Technology
author À.J.Mommersteeg				group /	
name Blade				format A4	drawing no. 008